

Entropy Adjusted Graphical Lasso for Sparse Precision Matrix Estimation

Vahe Avagyan*

January 10, 2025

Abstract

The estimation of a precision matrix is a crucial problem in various research fields, particularly when working with high dimensional data. In such settings, the most common approach is to use the penalized maximum likelihood. The literature typically employs Lasso, Ridge and Elastic Net norms, which effectively shrink the entries of the estimated precision matrix. Although these shrinkage approaches provide well-conditioned precision matrix estimates, they do not explicitly address the uncertainty associated with these estimated matrices. In fact, as the matrix becomes sparser, the precision matrix imposes fewer restrictions, leading to greater variability in the distribution, and thus, to higher entropy. In this paper, we introduce an entropy-adjusted extension of widely used Graphical Lasso using an additional log-determinant penalty term. The objective of the proposed technique is to impose sparsity on the precision matrix estimate and adjust the uncertainty through the log-determinant term. The advantage of the proposed method compared to the existing ones in the literature is evaluated through comprehensive numerical analyses, including both simulated and real-world datasets. The results demonstrate its benefits compared to existing approaches in the literature, with respect to several evaluation metrics.

Keywords: Elastic Net; Entropy adjustment; Gaussian Graphical Models; Lasso; Maximum Likelihood Estimation

*Biometris, Wageningen University and Research, Wageningen, The Netherlands

1 Introduction

Inverse of the covariance matrix (also known as precision matrix) has an important role in modern statistics and machine learning. Its accurate estimation is required in different research fields including finance (Choi et al., 2019), psychology (Till et al., 2023), genetics (Cai et al., 2013), brain studies (Huang et al., 2010), etc. The estimated precision matrix is fundamental in discriminant analysis, forecasting and several other statistical methodologies (McLachlan, 2004).

Precision matrix is closely related to the partial correlations among variables. Suppose the true precision matrix is $\Omega = [\omega_{ij}]_{1 \leq i, j \leq p} \in \mathbb{R}^{p \times p}$, which is positive definite. The entries of partial correlation matrix $P = [\rho_{ij}]_{1 \leq i, j \leq p}$ can be written in terms of the precision matrix entries:

$$\rho_{ij} = -\frac{\omega_{ij}}{\sqrt{\omega_{ii}\omega_{jj}}} \quad (1)$$

Therefore, the (i, j) entry of the precision matrix is zero if and only if the partial correlation of the variables X^i and X^j is zero. Under the assumption of multivariate normality, the entry $\omega_{ij} = 0$ of the precision matrix indicates the conditional independence between the variables X^i and X^j , given all the other variables (Dempster, 1972). In this way, the precision matrix is closely related to the Gaussian Graphical Models (GGM) which can represent the conditional independence of multivariate normally distributed variables in a convenient form as a graph (e.g., gene interaction networks). The GGM is an undirected graph defined as $G = (N, E)$. Here, the set of nodes $N = \{1, \dots, p\}$ represents the variables and the set of edges $E \subseteq N \times N$ consists of the pair indexes (i, j) corresponding to the ‘active’ entries $\omega_{ij} \neq 0$ for $1 \leq i, j \leq p$ (Lauritzen, 1996). The selection of GGM is an important problem in studying genetic interactions, human brain activity network, psychological networks, etc.

In recent decades, substantial research has focused on estimating the precision matrix under high dimensional settings. The most popular approach under high dimensional

settings is applying Lasso (Least absolute shrinkage and selection operator) or ℓ_1 norm penalty on an objective loss function. This approach is proposed in the regression context by Tibshirani (1996) and is widely used for estimating precision and covariance matrices. In particular, Banerjee et al. (2006) and Yuan and Lin (2007) independently proposed the ℓ_1 norm penalized log-likelihood maximization approach, also known as Graphical Lasso or GLasso estimator. Methods that employ ℓ_1 norm penalization include the Neighborhood Selection (Meinshausen and Bühlmann, 2006), Sparse Partial Correlation Estimation (Peng et al., 2009), constrained ℓ_1 norm minimization for inverse matrix estimation or CLIME (Cai et al., 2011), ℓ_1 norm penalized D-trace loss minimization (Zhang and Zou, 2014), Sparse Column-Wise Inverse Operator or SCIO (Liu and Luo, 2015), among several others. Despite the popularity of ℓ_1 norm penalty, other penalties (both convex and non-convex) are also considered, including Adaptive ℓ_1 norm (Fan et al., 2009; Avagyan et al., 2018), SCAD (Fan et al., 2009), Ridge or ℓ_2 norm (van Wieringen and Peeters, 2016; Kuismin et al., 2017; Bekker et al., 2023), Elastic-Net (Kovács et al., 2021; Bernardini et al., 2022), among others. We provide more details on estimation techniques in the next section.

In this article, we study the estimation of precision matrix Ω without assuming a specific structure or a sparsity pattern. In line with above-cited literature, our proposed method uses ℓ_1 norm penalized log-likelihood optimization problem. Although this penalty produces a sparse estimate, it can also lead to an increased uncertainty in capturing the true relationships between variables. This is particularly important when Lasso incorrectly shrinks some of the entries to zero. Moreover, Lasso penalization tends to shrink the eigenvalues of the estimated precision matrix. In general, smaller eigenvalues of a precision matrix correspond to higher uncertainty in the data structure. In order to diminish the induced uncertainty, we consider an additional log-determinant penalty on our optimization problem. This term is known as an appropriate measure of uncertainty in a context of multivariate normal distribution and is directly related to entropy (Anderson,

2003; Bishop and Nasrabadi, 2006). Our introduced method therefore induces sparsity through Lasso penalty term and adjusts uncertainty through the log-determinant term. The new augmented penalty is the convex combination of these two terms, motivated by the Elastic-Net penalization framework of Kovács et al. (2021) and Bernardini et al. (2022).

We evaluate the performances of the proposed estimator through an extensive numerical study. In particular, for our simulation analyses we consider different patterns (i.e., models) of the true precision matrix Ω , including those used in the experiments of the previous studies. We measure the performance of the considered methods in terms of statistical losses and GGM prediction measures. Finally, for the proposed method, we establish the convergence rate in the Frobenius norm under standard asymptotic theory (i.e., we assume that the number of variables is fixed).

The manuscript is organized as follows. In Section 2, we describe the related work and our proposed methodology. In Section 3, we evaluate the statistical performance of the proposed methodology and compare it with that of other approaches in the literature. In Section 4, we provide real data applications: classification of prostate cancer patients using Linear Discriminant Analysis and computation of an optimal financial portfolio. We provide our conclusions in Section 5. We demonstrate technical details in Appendix A, simulation models in Appendix B and additional numerical results in Appendix C. Finally, Appendix D develops the analytical convergence rate of the proposed method.

2 Methodology

2.1 Background and existing research

We use the following mathematical notations throughout this paper. For any symmetric matrix $\mathbf{A} = [a_{ij}]_{1 \leq i, j \leq p} \in \mathbb{R}^{p \times p}$, we denote the Frobenius or ℓ_2 norm by $\|\mathbf{A}\|_2 = \sqrt{\sum_{i=1}^p \sum_{j=1}^p a_{ij}^2}$, the ℓ_∞ norm by $\|\mathbf{A}\|_\infty = \max_{1 \leq i, j \leq p} |a_{ij}|$, the matrix ℓ_1 norm by $\|\mathbf{A}\|_{\ell_1} =$

$\max_{1 \leq j \leq p} \sum_{i=1}^p |a_{ij}|$, the elementwise ℓ_1 norm by $\|\mathbf{A}\|_1 = \sum_{i=1}^p \sum_{j=1}^p |a_{ij}|$, the spectral norm by $\|\mathbf{A}\|_{\text{sp}} = \sup_{\|x\|_2 \leq 1} \|\mathbf{A}x\|_2$. Here, we define the ℓ_2 norm by $\|\mathbf{a}\|_2 = \sqrt{\sum_{j=1}^p a_j^2}$ for any p -dimensional vector $\mathbf{a} = (a_1, \dots, a_p)^T \in \mathbb{R}^p$.

Without loss of generality, we assume that $\mathbf{X}_{n \times p}$ is mean-centered, observed sample data matrix, where each row $X_i = (X_{i1}, \dots, X_{ip})$ is a p -dimensional normal random vector, i.i.d. for $i = 1, \dots, n$ and has a covariance matrix $\Sigma = \Omega^{-1} \in \mathbb{R}^{p \times p}$. We define the sample covariance matrix as $S = \frac{1}{n} \sum_{i=1}^n X_i^T X_i = \frac{1}{n} \mathbf{X}^T \mathbf{X}$.

The estimation of a precision matrix under high dimensional settings has been widely studied in prior scholarly work. Among the proposed methods, the well-explored estimator is based on minimizing penalized (or constrained) negative log-likelihood function of a multivariate normal distribution. In particular, Graphical Lasso or GLasso (Banerjee et al., 2006; Yuan and Lin, 2007; Friedman et al., 2008) is the most popular approach for estimating the precision matrix and the corresponding GGM. This estimator is defined as:

$$\hat{\Omega}_{\text{GLasso}} = \arg \min_{\Omega} -\log \det(\Omega) + \text{trace}(\Omega S) + \gamma \|\Omega\|_1, \quad (2)$$

where the Lasso or ℓ_1 -norm penalty is used to encourage sparse solutions. Here, $\gamma > 0$ is the associated penalty (i.e., tuning or calibration) parameter that determines the degree of applied penalization on $\hat{\Omega}$. In case of GLasso, this parameter adjusts the accuracy and the sparsity of precision matrix estimator. When $\gamma = 0$, the problem (2) leads to the Maximum Likelihood Estimate of the covariance matrix $\hat{\Sigma} = S$.

Extant literature has studied the convergence rates of the GLasso precision matrix estimate $\hat{\Omega}_{\text{GLasso}}$ under certain assumptions. In particular, Rothman (2012) derived the convergence rate of the Glasso estimate in terms of Frobenius norm ℓ_2 , whereas Ravikumar et al. (2011) established the convergence rate in terms of ℓ_∞ and spectral norms. Moreover, Ravikumar et al. (2011) prove the model selection $\hat{\Omega}_{\text{Lasso}}$ consistency, i.e., show the estimate $\hat{\Omega}_{\text{Lasso}}$ specifies correctly the sparsity pattern of Ω , with probability converging to one.

In the context of penalization-driven approaches, a natural alternative to the Lasso penalization is the Ridge (or ℓ_2 -norm) penalization. The most straightforward version of this estimator is defined as:

$$\widehat{\Omega}_{\text{GRidge}} = \arg \min_{\Omega} -\log \det(\Omega) + \text{trace}(\Omega S) + \gamma \|\Omega\|_2^2. \quad (3)$$

This estimator was initially discussed by Witten and Tibshirani (2009) and Rothman (2012) and was further developed independently by van Wieringen and Peeters (2016) and Kuismin et al. (2017). Kuismin et al. (2017) refer to it as ROPE (Ridge-type Operator for the Precision matrix Estimation). On the other hand, van Wieringen and Peeters (2016) suggested an alternative Ridge-type estimator, defined as:

$$\widehat{\Omega}_{\text{T-GRidge}} = \arg \min_{\Omega} -\log \det(\Omega) + \text{trace}(\Omega S) + \frac{\gamma}{2} \|\Omega - T\|_2^2, \quad (4)$$

where $T \in \mathbb{R}^{p \times p}$ is a symmetric positive definite target matrix. Clearly, the penalty term of (3) is the special case of (4) with $T = \mathbf{0}$. Note that Ridge-type estimators are less complex than GLasso estimator (3) because they can be calculated by an explicit closed-form solutions. However, Ridge penalty does not induce exact sparsity on the estimated precision matrix, similar to Lasso penalty. In this way, these estimators are more attractive, if the sparsity of Ω is not an important property for the precision matrix estimate. For the sake of simplicity, analogously to the Graphical Lasso, we use the term Graphical Ridge (or GRidge) for the Ridge-type estimator (3) with no target, and Targeted Graphical Ridge (or T-GRidge) for the Ridge-type estimator (4) with a specified target.

More recently, scholarly work has studied the convex combination of Lasso and Ridge penalties. In the regression context, this penalty is known as Elastic-Net (Zou and Hastie, 2005). Bernardini et al. (2022) consider the following augmented estimation problem for estimating the precision matrix Ω :

$$\widehat{\Omega}_{\text{GEN}} = \arg \min_{\Omega} -\log \det(\Omega) + \text{trace}(\Omega S) + \gamma (\alpha \|\Omega\|_1 + (1 - \alpha) \|\Omega\|_2^2), \quad (5)$$

where the parameter $\alpha \in [0; 1]$ controls the balance between Lasso and Ridge penalization. For $\alpha = 1$, we have the Graphical Lasso approach (2), and for $\alpha = 0$, we have the Rope approach (4). Consistent with the terminology in regression context, this approach is called Graphical Elastic-Net (or GEN). The Elastic-Net penalization often brings the benefits of both Lasso and Ridge penalties: it leads to sparse estimators and simultaneously encourages stability in a presence of highly correlated variables.

Similar to the targeted Ridge penalization (4), Kovács et al. (2021) suggested a targeted version for the Elastic-Net penalty:

$$\begin{aligned} \widehat{\Omega}_{\text{T-GEN}} &= \arg \min_{\Omega} -\log \det(\Omega) + \text{trace}(\Omega S) \\ &+ \gamma \left(\alpha \|\Omega - T\|_1 + \frac{1 - \alpha}{2} \|\Omega - T\|_2^2 \right). \end{aligned} \quad (6)$$

Several target matrices are suggested in Kovács et al. (2021). The penalty term of (5) is a special case of (6) with $T = \mathbf{0}$, and the penalty term of (4) is a special case of (6) with $\alpha = 0$.

Note that the popularity of ℓ_1 and ℓ_2 norm penalties is due to their convexity. The literature also considers applying nonconcave penalties on the log-likelihood function, such as Smoothly Clipped Absolute Deviation or SCAD (Fan et al., 2009), ℓ_0 norm penalty (Marjanovic and Hero, 2015; Liu et al., 2016), ℓ_q norm penalty with $0 < q < 1$ (Marjanovic and Solo, 2014). For a further review on approaches for estimating high dimensional precision matrices, we refer to Fan et al. (2016).

2.2 Proposed methodology

Following the Elastic-Net-type penalization (5), we propose a new approach for estimating the precision matrix. Consider the following optimization problem:

$$\begin{aligned} \widehat{\Omega}_{\text{EAGL}} &= \arg \min_{\Omega} -\log \det(\Omega) + \text{trace}(\Omega S) \\ &+ \gamma \left(\alpha \|\Omega\|_1 + (1 - \alpha) \log \det(\Omega^{-1}) \right), \end{aligned} \quad (7)$$

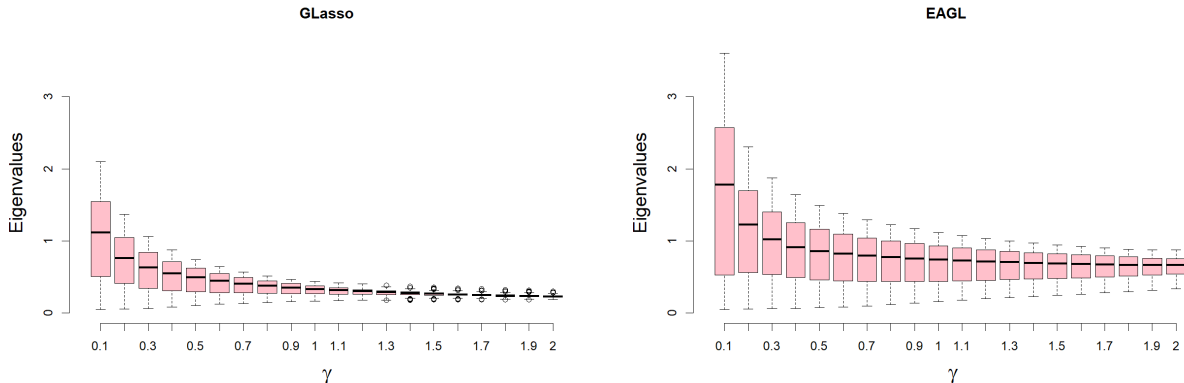
where $\alpha \in (0;1)$ is a combination parameter analogous to its use in the Elastic-Net penalization (5). The proposed approach is an augmented version of the GLasso method (2) with an additional $H_C(\mathbf{X}) = \log \det(\Omega^{-1}) = \log(\det(\Sigma))$ penalty term. Here, we still use the Lasso penalty, because our goal is to obtain a sparse estimate. The motivation behind the log det term is twofold.

First, we can show that this term represents the entropy of multivariate Gaussian distribution, up to an additive constant. We show this in Appendix A. In the context of machine learning and statistics, entropy is viewed as a measure of uncertainty or randomness within a dataset. High entropy indicates more randomness, while low entropy suggests a more organized data and thus, better measurability of the relationships among the variables. The objective of the proposed technique is therefore to impose sparsity on the precision matrix estimate while adjusting the overall uncertainty, which leads to a more efficient estimate.

Second, the term $H_C(\mathbf{X})$ produces an additional calibration for the eigenvalues of estimated precision matrix. Note that $H_C(\mathbf{X}) = \log \det(\Omega^{-1}) = -\sum_{i=1}^p \log(\lambda_i)$, where λ_i is the i -th eigenvalue of the precision matrix Ω . The additional log det penalty forces the precision matrix eigenvalues to shrink less which occurs due to the Lasso penalization (such shrinkage pattern is in line with the findings by Friedman et al. (2008) and Avagyan (2021)). As a result, the eigenvalues of the estimated precision matrix $\widehat{\Omega}_{\text{EAGL}}$ become higher and less shrunk than those of $\widehat{\Omega}_{\text{GLasso}}$. In Figure 1, we provide a simple example, which shows the distribution of eigenvalues of $\widehat{\Omega}_{\text{GLasso}}$ and $\widehat{\Omega}_{\text{EAGL}}$ for different values of the penalization parameter γ from a sequence varying from 0.1 to 2. For the data simulation, we use the settings described in Section 3 and we assume that the true precision matrix has a structure given in Model 1 for $p = 200$ and $n = 100$. We can clearly see that the eigenvalues of $\widehat{\Omega}_{\text{EAGL}}$ shrink slower than those of $\widehat{\Omega}_{\text{GLasso}}$. Therefore, we can expect a more accurate eigenspectrum of the estimated precision matrix with the additional penalty term.

Note that large precision matrix eigenvalues indicate strong concentration in the prin-

Figure 1: Eigenvalues of GLasso (left) and EAGL (right) estimators for different value of the penalty parameter γ .



principal axes and thus, lower uncertainty. This behavior aligns with the intuition that as the matrix becomes sparser due to the Lasso penalization, it reflects to fewer restrictions on the relationships between the variables (i.e., many variables become conditionally independent given the others). This will lead to a greater variability in the joint distribution (i.e., it will be more spread out) and, consequently, to a higher entropy.

The use of log det penalty is not new in the literature for other purposes. For example, a similar log det penalty is used by Rothman (2012) for estimating sparse covariance matrix. However, this penalty was used as a logarithmic barrier to ensure that the obtained estimator is positive definite. To the best of our knowledge, this term has not been used in the context of entropy adjustment.

We call the proposed approach *Entropy Adjusted Graphical Lasso* or EAGL. Note that when $\alpha = 1$, the problem (7) reduces to (2). Interestingly, when $\alpha = 0$, the problem (7) leads to the covariance matrix estimator $\hat{\Sigma} = \frac{1}{1 + \gamma}S$, which is a special case of the James-Stein estimator (James and Stein, 1992) and has a better performance than the traditional estimator $\hat{\Sigma} = S$ in terms of the MSE (see also Haff, 1980, for a similar covariance estimator). This estimator can also be seen as the Ledoit-Wolf shrinkage covariance estimator (Ledoit and Wolf, 2004) towards a zero target.

Remark: Following the targeted version of the Elastic-Net estimator (5), we can also

employ an additional target matrix T in the Lasso penalty. However, in this paper we focus on the analysis of EAGL estimator without using target matrices.

3 Simulation analysis

In this section, we evaluate the numerical performance of the proposed method using simulated data. The data generation process is based on different scenarios (i.e., models) for the true precision matrix Ω . Specifically, we consider several popular methods for estimating the precision matrix. We compare our proposed estimator EAGL with Graphical Lasso, Graphical Elastic-Net (with and without a target), Graphical Ridge (with and without a target) and Graphical SCAD. Our study is implemented in **R** using the following packages: `glassoFast` for EAGL and `GLasso`, `GLassoElnetFast` for Graphical Elastic-Net estimators, `rope` for Graphical Ridge estimators, `ggmncv` for Graphical SCAD. All packages are available at <http://cran.r-project.org/web/packages>. Following Kuismin et al. (2017), we use scalar matrix $T = \nu \mathbf{I}$ for the target matrix, which is used in all targeted estimators (here, $\nu = p/\text{trace}(S)$ and $\mathbf{I} \in \mathbb{R}^{p \times p}$ is identity matrix). As indicated earlier, Graphical Ridge approaches do not provide sparse estimators. Therefore, we perform an additional sparsification on these estimates using `sparsify()` function of `rags2ridges` package, with ‘localFDR’ thresholding argument (see Peeters et al., 2022, for more details).

3.1 Performance evaluation

We evaluate the performance of a precision matrix estimator based on several popular statistical distances and errors. We consider the relative entropy losses, such as the Kullback-Leibler loss and the Reverse Kullback-Leibler loss (see, for instance, Yuan, 2010; Yin and Li, 2013; Avagyan, 2021, etc.), the Relative Trace Error (RTE) and matrix losses, such as the Frobenius ℓ_2 norm, the spectral ℓ_{sp} norm and the matrix ℓ_1 norm (see, for instance, Cai

et al., 2011; Zhang and Zou, 2014; van Wieringen and Peeters, 2016, etc.). These measures are defined as:

$$\begin{aligned}
\text{KLL}(\widehat{\Omega}, \Omega) &= \text{trace}(\Omega^{-1}\widehat{\Omega}) - \log \det(\Omega^{-1}\widehat{\Omega}) - p, \\
\text{RKLL}(\widehat{\Omega}, \Omega) &= \text{trace}(\Omega\widehat{\Omega}^{-1}) - \log \det(\Omega\widehat{\Omega}^{-1}) - p, \\
\text{RTE}(\widehat{\Omega}, \Omega) &= \left| 1 - \frac{\text{trace}(\widehat{\Omega})}{\text{trace}(\Omega)} \right| \\
\ell_2(\widehat{\Omega}, \Omega) &= \|\widehat{\Omega} - \Omega\|_2, \\
\ell_{\text{sp}}(\widehat{\Omega}, \Omega) &= \|\widehat{\Omega} - \Omega\|_{\text{sp}}, \\
\ell_1(\widehat{\Omega}, \Omega) &= \|\widehat{\Omega} - \Omega\|_{\ell_1}.
\end{aligned}$$

Furthermore, we evaluate the graphical modeling (i.e., sparsity pattern prediction of the GGM) based on overall summary metrics: Matthews Correlation Coefficient (Matthews, 1975) and Balanced Accuracy (Brodersen et al., 2010). These metrics are respectively defined as:

$$\begin{aligned}
\text{MCC} &= \frac{\text{TP} \times \text{TN} - \text{FP} \times \text{FN}}{\sqrt{(\text{TP} + \text{FP})(\text{TP} + \text{FN})(\text{TN} + \text{FP})(\text{TN} + \text{FN})}}, \\
\text{BA} &= \frac{1}{2} \left(\frac{\text{TP}}{\text{TP} + \text{FN}} + \frac{\text{TN}}{\text{TN} + \text{FP}} \right).
\end{aligned}$$

Here, TP is the number of correctly selected non-zero entries (i.e., true positives), TN is the number of correctly selected zero entries (i.e., true negatives), FP is the number of incorrectly selected non-zero entries (i.e., false positives), and FN is the number of incorrectly selected zero entries (i.e., false negatives). In case of MCC, the coefficient of 1 and -1 indicate the perfect and the worst classification, respectively. In case of the Balanced Accuracy, the coefficient 1 indicates the perfect selection, whereas the coefficient 0 indicates the worst selection. For convenience, we further rescale the MCC to the range of the Balanced Accuracy.

$$\text{uMCC} = \frac{\text{MCC} + 1}{2}.$$

Both metrics are popular techniques in statistics and machine learning as standard accuracy metrics for evaluating binary classifications (see Chicco and Jurman, 2020, for more details).

3.2 Simulation settings

We generate multivariate normal random samples with zero mean and covariance matrix $\Sigma = \Omega^{-1}$. The following models are considered for the true precision matrix $\Omega = [\omega_{ij}]_{1 \leq i, j \leq p}$:

- **Model 1.** Band matrix, with $\omega_{ii} = 1$, $\omega_{i,i-1} = \omega_{i-1,i} = 0.45$ and other values are 0 (Yuan and Lin, 2007; Friedman et al., 2008, etc.)
- **Model 2.** Band matrix, with $\omega_{ii} = 1$, $\omega_{i,i-1} = \omega_{i-1,i} = 0.5$, $\omega_{i,i-2} = \omega_{i-2,i} = 0.35$ and other values are 0 (Kuismin et al., 2017; Avagyan, 2021).
- **Model 3.** A block-diagonal matrix, with four equally sized blocks along the diagonal. Each block is defined as $\omega_{ij} = 0.6^{|i-j|}$ (Cai et al., 2011; Fan et al., 2009, etc.)
- **Model 4.** A random positive definite matrix, with approximately 50% of non-zero entries. This matrix is generated using Matlab command `sprandsym` with a parameter 0.5 (Avagyan, 2021).
- **Model 5.** Erdős-Rényi random graph. We define $\Theta = [\theta_{ij}]_{1 \leq i, j \leq p}$, with $\theta_{ij} = u_{ij}\delta_{ij}$, where $u_{ij} = u_{ji}$ is a uniform random variable on an interval $[0.4, 0.8]$ and $\delta_{ij} = \delta_{ji}$ is a Bernoulli random variable with a success probability 0.05. Next, we take $\Omega = \Theta + (|\lambda_{\min}(\Theta) + 0.05|)\mathbf{I}$, where $\lambda_{\min}(\Theta)$ is the smallest eigenvalue of Θ (Kovács et al., 2021).
- **Model 6.** Scale-free graph, based on the Barabási–Albert algorithm. The resulting graph has p edges. This matrix is generated using R package `huge` (Kovács et al., 2021; Bernardini et al., 2022).

- **Model 7.** Hub graph with 10 hubs, each hub containing $p/20$ nodes. The resulting graph has $p - 10$ edges. This matrix is generated using R package `huge` with parameters $\nu = 0.3$ and $u = 0.1$ (Kovács et al., 2021; Bernardini et al., 2022).

The generated matrices are further standardized to have unit diagonal. We provide the graphical models corresponding to each considered precision matrix structure in Appendix B. Finally, we set the sample size $n = 100$ and the number of variables $p = 200$. The number of replications is 100.

3.3 Penalty parameter selection

Selecting the penalty parameter is a crucial step for any penalized optimization problem. In our numerical analysis, we select the penalty parameter γ using 5-fold Cross-Validation or CV (Bien and Tibshirani, 2011) approach. This is a commonly used technique in precision matrix estimation methods and is consistent with studies of Kovács et al. (2021), Kuismin et al. (2017), etc. Following Bernardini et al. (2022) and Kovács et al. (2021), we set $\alpha = 0.5$ for the estimators GEN, T-GEN and the proposed EAGL.

Another popular technique for estimating the penalty parameter of the precision matrix estimation methods is Bayesian Information Criterion or BIC (Yuan and Lin, 2007). In this paper, we put CV above BIC, because CV leads to lower statistical losses. However, according to Wasserman and Roeder (2009), CV may provide many false positives compared to BIC. Following Bernardini et al. (2022), we conduct additional analyses for demonstrating the performance of our proposed methodology where the penalty parameter γ is selected using BIC approach. We provide these results in Appendix C. These findings provide further insights into the comparison of the two selection techniques.

3.4 Computational time

Table 1 shows the average computational time required for each method. The reported time includes the required time to select the penalty parameter γ using CV and the required time to run the method. We assume that the true precision matrix has a structure given in Model 1 for $p = 200$ and $n = 100$. The analyses are performed on Intel Core i7-1280P CPU, 1.80 GHz. The computational time of EAGL is relatively low, compared to the other methods. Note that, in general, Ridge-type approaches are not complex and require little computation (usually less than a second). However, the time provided in Table 1 is high due to the sparsification procedure.

Table 1: Average computational time (in seconds) for different methods.

$\hat{\Omega}_{\text{GLasso}}$	$\hat{\Omega}_{\text{GEN}}$	$\hat{\Omega}_{\text{T-GEN}}$	$\hat{\Omega}_{\text{GRidge}}$	$\hat{\Omega}_{\text{T-GRidge}}$	$\hat{\Omega}_{\text{SCAD}}$	$\hat{\Omega}_{\text{EAGL}}$
2.88	5.44	4.36	13.1	12.6	2.73	1.86

3.5 Discussion of results

Tables 5-11 report the averages of the measures over 100 replications. Corresponding standard deviations are provided in the parentheses. First, we observe that EAGL outperforms GLasso in terms of RKLL, RTE, ℓ_2 , ℓ_{sp} and ℓ_1 norms for all models, in terms of KLL for models 1, 3, 6 and 7, and in terms of uMCC for models 1, 2, 3, and 7. On the other hand, GLasso method performs better than EAGL in terms of KLL for models 2, 4 and 5 and in terms of uMCC for models 4, 5 and 6. Table 2 provides a summary for the comparison between EAGL and GLasso estimators, indicating scenarios, where EAGL outperforms GLasso.

Tables 5 - 11 about here.

Comparing our proposed method with other methods, we see that in general EAGL provides better results, especially in terms of the statistical losses. However, SCAD provides the best overall results in terms of the KLL for models 1, 2, 3, 4, in terms of the ℓ_1 norm for model 7 and in terms of uMCC for model 5. We observe that T-GEN estimator provides the best overall results in terms of KLL for models 5 and 6, in terms of ℓ_2 norm in terms for model 6, in terms of the ℓ_1 norm for model 6 and in terms of BA for model 4 and 5. On the other hand, GEN estimator provides the best overall results in terms of BA for model 6. T-GRidge estimator provides the best overall results in terms of the ℓ_1 norm for model 3, in terms of BA for model 1 and in terms of uMCC for model 7. Finally, GRidge estimator provides the best overall results in terms of the ℓ_1 norm for models 1 and 2, in terms of uMCC for models 1, 2, 3 and 6.

Table 2: EAGL (✓) vs GLasso (X): A Comparative Overview.

Metrics	Models						
	1	2	3	4	5	6	7
KLL	✓	X	✓	X	X	✓	✓
RKLL	✓	✓	✓	✓	✓	✓	✓
ℓ_2	✓	✓	✓	✓	✓	✓	✓
ℓ_{sp}	✓	✓	✓	✓	✓	✓	✓
ℓ_1	✓	✓	✓	✓	✓	✓	✓
RTE	✓	✓	✓	✓	✓	✓	✓
uMCC	✓	✓	✓	✓	✓	✓	✓
BA	✓	✓	✓	X	X	X	✓

In sum, the proposed EAGL estimator in general provides favorable performance than GLASSO, GEN, T-GEN, GRidge, T-GRidge and SCAD methods for most of the models

in terms of most statistical losses and GGM prediction measures. Moreover, EAGL shows a suitable trade-off between the matrix prediction and sparsity pattern identification, i.e., the outperformance in terms of one criterion does not diminish the other one. This suggests that entropy adjustment enhances both the statistical accuracy of the estimated precision matrix and the performance of GGM selection.

In addition, we conduct the same study where the penalty parameter is selected using BIC (see Appendix C). The results support our discussion above and the comparison of the considered methods remains comparatively the same.

4 Real data application

In this section, we conduct an empirical analysis of the proposed method through two real-data applications. The first application aims at predicting prostate cancer patients and the second one aims at selecting a large financial portfolio.

4.1 Prostate cancer study

In this application, we focus on the problem of predicting prostate cancer patients using Linear Discriminant Analysis (LDA) with different precision matrix estimates. We use a dataset analysed by Singh et al. (2002), which contains measurements of the gene expression levels of 6033 genes for 102 specimens. Out of these specimens, 52 are taken from prostate cancer patients, and 50 are taken from healthy patients. The dataset `singh2002` is available in R package `sda`.

In order to evaluate the performance of the proposed EAGL method, we first divide the data into a training set and a testing set with sizes 60 and 42, respectively. Second, for the training set we apply two sample t-test between the two groups (cancer and healthy) in order to select the most significant 100 genes with the smallest p-values. Based on the selected genes, we obtain the estimated precision matrix $\hat{\Omega}$ using the methods considered

in section 3. The penalty parameters are estimated using the 5-fold CV technique. The estimated precision matrix is then used in the following LDA procedure.

Let's assume $\boldsymbol{\mu}_1$ and $\boldsymbol{\mu}_2$ are the population means of the gene expression levels for cancer and healthy patients, respectively, and Ω is the corresponding population precision matrix. We use Mahalanobis distance $\mathbf{a}^T(\mathbf{x} - \boldsymbol{\mu})$, where $\mathbf{a} = \Omega(\boldsymbol{\mu}_1 - \boldsymbol{\mu}_2)$ and $\boldsymbol{\mu} = \frac{\boldsymbol{\mu}_1 + \boldsymbol{\mu}_2}{2}$. We estimate the means $\boldsymbol{\mu}_1$ and $\boldsymbol{\mu}_2$ using within group averages $\bar{\mathbf{x}}_1$ and $\bar{\mathbf{x}}_2$, respectively, calculated with the training data. Next, we assign the testing observation \mathbf{x} to the cancer group if $\hat{\mathbf{a}}^T(\mathbf{x} - \hat{\boldsymbol{\mu}}) > 0$, where $\hat{\mathbf{a}} = \hat{\Omega}(\bar{\mathbf{x}}_1 - \bar{\mathbf{x}}_2)$ and $\hat{\boldsymbol{\mu}} = \frac{\bar{\mathbf{x}}_1 + \bar{\mathbf{x}}_2}{2}$. We repeat this process 100 times and calculate the missclassification rate for each precision matrix estimator. In addition, we calculate the uMCC and BA scores, where we assume that TP and TN are the number of correctly predicted cancer and healthy patients, respectively, and FP and FN are the number of incorrectly classified cancer and healthy patients, respectively.

Table 3 reports the average prediction measures for each method. We observe that the proposed EAGL shows lower missclassification rate and higher uMCC and BA than the GLasso, GEN, GRidge, T-Gridg and SCAD estimators. We observe that EAGL and the targeted T-GEN have roughly the same classification measures. However, we note that in contrast to the T-GEN approach, the proposed EAGL approach does not require selecting a target matrix and is computationally more efficient.

Table 3: Average classification measures over 100 replications.

	$\hat{\Omega}_{\text{GLasso}}$	$\hat{\Omega}_{\text{GEN}}$	$\hat{\Omega}_{\text{T-GEN}}$	$\hat{\Omega}_{\text{GRidge}}$	$\hat{\Omega}_{\text{T-GRidge}}$	$\hat{\Omega}_{\text{SCAD}}$	$\hat{\Omega}_{\text{EAGL}}$
Missclassification rate	0.168	0.178	0.123	0.155	0.149	0.134	0.128
uMCC	0.834	0.825	0.879	0.848	0.854	0.868	0.873
BA	0.831	0.822	0.876	0.845	0.851	0.865	0.871

4.2 S&P 500 portfolio optimization

In our second application, we focus on developing an optimal stock portfolio with minimum risk (Goto and Xu, 2015; Avagyan and Mei, 2022; Bernardini et al., 2022). Note that estimating the precision matrix has a crucial role in computing optimal portfolio weights (see Stevens, 1998, for more details). In the mean-variance optimization, the risk of a p -dimensional (global) portfolio $w = (w_1, \dots, w_p)$ is measured by the standard deviation of its returns, given as $\sqrt{w^T \Sigma w}$ (Markowitz, 1952), where Σ is the global covariance matrix. In the absence of short-sale constraints, the estimated weights \hat{w}_{MVP} of the single-period minimum variance portfolio are defined as:

$$\begin{aligned} \hat{w}_{MVP} &= \arg \min_w w^T \hat{\Sigma} w \\ &\text{subject to } w^T \mathbf{1} = 1, \end{aligned} \tag{8}$$

where $\mathbf{1}$ is a p -dimensional vector of ones. DeMiguel et al. (2009a) demonstrate that the minimum variance optimization problem has an explicit solution, defined as:

$$\hat{w}_{MVP} = \frac{\hat{\Sigma}^{-1} \mathbf{1}}{\mathbf{1}^T \hat{\Sigma}^{-1} \mathbf{1}}. \tag{9}$$

This means that the minimum variance portfolio depends on the precision matrix estimate $\hat{\Omega} = \hat{\Sigma}^{-1}$. Therefore, we expect that an accurate estimate of the precision matrix will lead to a better portfolio.

We use historical monthly returns of $p = 267$ stock constituents of S&P 500 index for a total of $n = 364$ months, covering the period from January 1991 to April 2021. The constituents come from 11 major market sectors. The dataset is available at the **R** package `probstats4econ`. Following Ledoit and Wolf (2004), we assume that stock returns are independent and identically distributed. In order to evaluate the performance of selected portfolio, we perform the ‘rolling-horizon’ procedure of DeMiguel et al. (2009a). First, we select a rolling window with length $m = 150$ months, which is used to estimate the precision matrix Ω and the corresponding portfolio weights. Next, we compute the out-of-sample

portfolio returns of the next period. This procedure is repeated $n - m$ times by including the returns of next period and dropping the earliest one (thus, keeping the rolling window with the same size). Finally, we evaluate the performance of the portfolio by computing the out-of-sample mean (i.e., reward), the standard deviation (i.e., risk) and the Sharpe Ratio, based on the obtained $n - m$ out-of-sample returns \hat{R}_t :

$$\hat{\mu} = \frac{1}{n - m} \sum_{t=m}^{n-1} \hat{R}_{t+1}, \quad (10)$$

$$\hat{\sigma}^2 = \frac{1}{n - m - 1} \sum_{t=m}^{n-1} (\hat{R}_{t+1} - \hat{\mu})^2, \quad (11)$$

$$\widehat{\text{SR}} = \frac{\hat{\mu}}{\hat{\sigma}}. \quad (12)$$

The Sharpe Ratio, also known as the reward-to-risk ratio, measures the performance of a portfolio relative to its associated risk. A higher Sharpe Ratio indicates better investment performance in terms of risk-adjusted returns.

In our analysis, in addition to the selected methods, we also evaluate the performance of two alternatives, commonly used in the literature. The first one is the inverse of Ledoit-Wolf covariance estimator $\hat{\Omega}_{\text{LW}} = \hat{\Sigma}_{\text{LW}}^{-1}$ (Ledoit and Wolf, 2004), which is a popular approach for selecting an optimal financial portfolio. The second one is the naive approach $\hat{\Omega}_{\text{Naive}} = \mathbf{I}$, which leads to allocating $1/p$ weight of wealth to each of the p assets available for investment (DeMiguel et al., 2009b).

Table 4 presents the out-of-sample performances for portfolios obtained using different precision matrix estimates. The penalty parameter γ is selected using 5-fold CV technique. First, our results show that the proposed EAGL method provides the lowest out-of-sample portfolio risk. EAGL, GLASSO and LW estimators lead to the highest out-of-sample mean (i.e., reward) compared to all the other methods. Finally, our proposed approach demonstrate the highest Sharpe Ratio. This means that the portfolios obtained using the proposed precision matrix estimate are the most efficient in terms of the risk-adjusted return. The results show that the naive approach provides the lowest out-of-sample mean

and the highest risk. Finally, despite its popularity, the LW estimator leads to relatively high risk.

Table 4: Out-of-sample performance (rounded) for different estimation methods.

	$\widehat{\Omega}_{\text{GLasso}}$	$\widehat{\Omega}_{\text{GEN}}$	$\widehat{\Omega}_{\text{T-GEN}}$	$\widehat{\Omega}_{\text{GRidge}}$	$\widehat{\Omega}_{\text{T-GRidge}}$	$\widehat{\Omega}_{\text{SCAD}}$	$\widehat{\Omega}_{\text{LW}}$	$\widehat{\Omega}_{\text{Naive}}$	$\widehat{\Omega}_{\text{EAGL}}$
Mean	0.015	0.014	0.014	0.014	0.012	0.013	0.015	0.012	0.015
Risk	0.036	0.036	0.038	0.038	0.041	0.037	0.039	0.045	0.034
Sharpe Ratio	0.420	0.400	0.386	0.385	0.293	0.364	0.383	0.279	0.438

In addition to the out-of-sample performance above, we also examine the interaction structure between the companies. For demonstrative purposes, we apply our proposed EAGL approach on the whole data. We observe that the partial correlation matrix (not shown), corresponding to the precision matrix, is roughly block-diagonal, where each block represents a market sectors. The interactions (i.e., partial correlations) are stronger among the companies within each sector. This indicates that there is a strong community structure, with communities made up of companies from the same sector. Figure 2 demonstrates the Gaussian Graphical Model illustrating the interactions among the companies. The GGM reveals groups of nodes (i.e., companies) such that within group interactions are stronger and more frequent than between group interactions.

Figure 2 about here.

5 Conclusions

In this article, we introduce a novel method for estimating sparse precision matrices in high dimensional settings. The proposed approach is an augmented version of the popular Graphical Lasso method, which incorporates Lasso penalization framework with an addi-

tional log-determinant penalty. This combined penalty allows for entropy adjustment of the multivariate Gaussian distribution, thereby reducing the uncertainty.

Through extensive numerical analyses, using both simulated and real datasets, we demonstrate that the proposed entropy adjustment helps achieve better performance of the estimated precision matrix without increasing the computational costs. We evaluate our method using different loss functions and prediction performance measures. Our method provides lower statistical losses and better model selection metrics for Gaussian Graphical Models compared to other established approaches in the literature. We calibrate the penalty parameter using 5-fold Cross-Validation and BIC, ensuring practical usability across different datasets. Our proposed approach does not rely on the selection of a target matrix, though it can be extended to include a target matrix in the Lasso norm. Finally, we establish the convergence rate of the proposed EAGL estimator in the Frobenius norm under standard asymptotic conditions.

For researchers, we suggest incorporating the proposed EAGL in situations, where uncertainty reduction and sparsity are of high importance. This recommendation is particularly pertinent for scholars and practitioners who employ the precision matrix in finance, discriminant analysis and network modeling, because the improved accuracy of the estimated precision matrix can significantly improve their analyses.

While our methodology has notable advantages, it is important to acknowledge certain limitations. First, in our study, we choose $\alpha = 0.5$, i.e., halfway between Lasso and log det penalties. However, the optimal value for α may differ from this choice. Second, α should be sufficiently far from zero, because EAGL estimate does not exist for $\alpha = 0$, when p is close to or exceeds n . Finally, we may encounter some convergence problems for EAGL for a relatively large norm of the true covariance matrix.

Our results pave the way for future research. First, future research should further investigate the role of parameter α on numerical and theoretical performance of our methodology.

Second, it might be interesting to explore the relationship between the parameters γ and α in greater detail. Third, a promising research direction involves applying the proposed entropy adjustment to other precision matrix estimators, such as the Entropy Adjusted Graphical Ridge. Finally, studying the proposed estimator from a Bayesian perspective could provide valuable insights and deepen our understanding of its theoretical properties.

Despite the limitations, we hope our paper contributes valuable insights into precision matrix estimation and stimulates future research in this area.

Table 5: Average measures (with standard deviations) over 100 replications for Model 1.

Bold letters indicate the best results.

	$\widehat{\Omega}_{\text{GLasso}}$	$\widehat{\Omega}_{\text{GEN}}$	$\widehat{\Omega}_{\text{T-GEN}}$	$\widehat{\Omega}_{\text{GRidge}}$	$\widehat{\Omega}_{\text{T-GRidge}}$	$\widehat{\Omega}_{\text{SCAD}}$	$\widehat{\Omega}_{\text{EAGL}}$
KLL	27.56 (0.930)	33.08 (0.627)	30.86 (0.541)	58.14 (1.399)	64.03 (2.624)	21.00 (0.591)	23.61 (0.839)
RKLL	38.30 (2.767)	49.72 (1.681)	45.20 (0.918)	75.97 (0.832)	87.32 (5.451)	25.49 (0.745)	22.77 (0.845)
ℓ_2	7.493 (0.401)	8.365 (0.191)	8.193 (0.047)	9.994 (0.019)	10.40 (0.201)	6.318 (0.078)	6.107 (0.153)
ℓ_{sp}	1.041 (0.039)	1.126 (0.019)	1.105 (0.013)	1.253 (0.010)	1.308 (0.025)	0.927 (0.023)	0.891 (0.023)
ℓ_1	1.654 (0.084)	1.775 (0.066)	1.688 (0.053)	1.356 (0.026)	1.395 (0.029)	1.467 (0.068)	1.403 (0.068)
RTE	0.369 (0.030)	0.419 (0.015)	0.410 (0.003)	0.482 (0.001)	0.495 (0.015)	0.297 (0.005)	0.256 (0.010)
uMCC	0.653 (0.011)	0.634 (0.002)	0.648 (0.002)	0.979 (0.007)	0.955 (0.018)	0.681 (0.003)	0.704 (0.004)
BA	0.936 (0.009)	0.919 (0.002)	0.933 (0.002)	0.990 (0.006)	0.990 (0.008)	0.955 (0.002)	0.965 (0.001)

Table 6: Average measures (with standard deviations) over 100 replications for Model 2.

Bold letters indicate the best results.

	$\widehat{\Omega}_{\text{GLasso}}$	$\widehat{\Omega}_{\text{GEN}}$	$\widehat{\Omega}_{\text{T-GEN}}$	$\widehat{\Omega}_{\text{GRidge}}$	$\widehat{\Omega}_{\text{T-GRidge}}$	$\widehat{\Omega}_{\text{SCAD}}$	$\widehat{\Omega}_{\text{EAGL}}$
KLL	45.05 (1.137)	47.27 (0.629)	46.80 (0.706)	69.07 (1.931)	77.36 (0.849)	42.08 (1.267)	46.07 (1.135)
RKLL	77.94 (6.640)	84.77 (0.981)	85.06 (3.230)	106.7 (3.601)	162.0 (2.687)	63.59 (5.960)	58.75 (1.691)
ℓ_2	11.92 (0.393)	12.17 (0.029)	12.29 (0.180)	13.15 (0.085)	14.31 (0.040)	11.27 (0.374)	11.21 (0.147)
ℓ_{sp}	1.954 (0.054)	1.984 (0.010)	2.002 (0.025)	2.096 (0.014)	2.247 (0.006)	1.875 (0.054)	1.867 (0.023)
ℓ_1	2.683 (0.067)	2.773 (0.043)	2.695 (0.050)	2.250 (0.027)	2.325 (0.014)	2.602 (0.058)	2.547 (0.060)
RTE	0.467 (0.028)	0.484 (0.002)	0.489 (0.013)	0.493 (0.007)	0.573 (0.005)	0.412 (0.026)	0.366 (0.010)
uMCC	0.671 (0.011)	0.651 (0.002)	0.668 (0.006)	0.873 (0.008)	0.827 (0.007)	0.689 (0.009)	0.703 (0.007)
BA	0.919 (0.010)	0.900 (0.002)	0.917 (0.005)	0.829 (0.016)	0.795 (0.014)	0.933 (0.005)	0.940 (0.004)

Table 7: Average measures (with standard deviations) over 100 replications for Model 3.

Bold letters indicate the best results.

	$\widehat{\Omega}_{\text{GLasso}}$	$\widehat{\Omega}_{\text{GEN}}$	$\widehat{\Omega}_{\text{T-GEN}}$	$\widehat{\Omega}_{\text{GRidge}}$	$\widehat{\Omega}_{\text{T-GRidge}}$	$\widehat{\Omega}_{\text{SCAD}}$	$\widehat{\Omega}_{\text{EAGL}}$
KLL	37.53 (0.736)	40.05 (0.420)	37.814 (0.401)	51.628 (0.608)	56.159 (0.231)	34.445 (0.673)	37.047 (0.778)
RKLL	86.52 (5.332)	95.22 (1.214)	92.807 (1.594)	155.85 (2.930)	144.915 (2.111)	72.145 (3.845)	61.52 (0.917)
ℓ_2	14.87 (0.214)	15.10 (0.028)	15.218 (0.044)	16.479 (0.043)	16.312 (0.033)	14.396 (0.166)	13.93 (0.047)
ℓ_{sp}	3.249 (0.033)	3.280 (0.008)	3.299 (0.008)	3.477 (0.007)	3.448 (0.005)	3.180 (0.026)	3.096 (0.011)
ℓ_1	3.849 (0.078)	3.942 (0.051)	3.673 (0.043)	3.602 (0.014)	3.525 (0.008)	3.758 (0.064)	3.601 (0.057)
RTE	0.495 (0.018)	0.514 (0.003)	0.515 (0.005)	0.603 (0.005)	0.523 (0.006)	0.447 (0.015)	0.359 (0.005)
uMCC	0.538 (0.005)	0.532 (0.004)	0.550 (0.004)	0.599 (0.001)	0.594 (0.001)	0.543 (0.004)	0.550 (0.004)
BA	0.527 (0.003)	0.527 (0.003)	0.528 (0.002)	0.526 (0.001)	0.524 (0.001)	0.528 (0.002)	0.528 (0.002)

Table 8: Average measures (with standard deviations) over 100 replications for Model 4.

Bold letters indicate the best results.

	$\widehat{\Omega}_{\text{GLasso}}$	$\widehat{\Omega}_{\text{GEN}}$	$\widehat{\Omega}_{\text{T-GEN}}$	$\widehat{\Omega}_{\text{GRidge}}$	$\widehat{\Omega}_{\text{T-GRidge}}$	$\widehat{\Omega}_{\text{SCAD}}$	$\widehat{\Omega}_{\text{EAGL}}$
KLL	92.70 (1.535)	95.88 (0.995)	95.19 (1.002)	135.1 (2.476)	135.4 (1.873)	91.84 (1.019)	107.9 (1.891)
RKLL	259.6 (22.24)	267.8 (1.860)	261.9 (1.884)	289.5 (8.626)	357.9 (2.342)	264.4 (10.01)	155.8 (4.080)
ℓ_2	17.26 (0.205)	17.41 (0.013)	17.36 (0.014)	17.78 (0.054)	18.23 (0.011)	17.28 (0.107)	15.94 (0.077)
ℓ_{sp}	5.291 (0.024)	5.291 (0.008)	5.287 (0.008)	5.236 (0.008)	5.292 (0.005)	5.303 (0.014)	5.150 (0.017)
ℓ_1	10.11 (0.061)	10.11 (0.056)	10.10 (0.057)	10.01 (0.045)	10.10 (0.039)	10.11 (0.056)	9.913 (0.080)
RTE	0.654 (0.017)	0.678 (0.002)	0.672 (0.002)	0.713 (0.005)	0.752 (0.001)	0.649 (0.010)	0.481 (0.006)
uMCC	0.597 (0.003)	0.597 (0.003)	0.598 (0.003)	0.591 (0.002)	0.594 (0.002)	0.598 (0.003)	0.598 (0.003)
BA	0.580 (0.003)	0.583 (0.003)	0.583 (0.003)	0.532 (0.001)	0.536 (0.002)	0.578 (0.002)	0.578 (0.003)

Table 9: Average measures (with standard deviations) over 100 replications for Model 5.

Bold letters indicate the best results.

	$\hat{\Omega}_{\text{GLasso}}$	$\hat{\Omega}_{\text{GEN}}$	$\hat{\Omega}_{\text{T-GEN}}$	$\hat{\Omega}_{\text{GRidge}}$	$\hat{\Omega}_{\text{T-GRidge}}$	$\hat{\Omega}_{\text{SCAD}}$	$\hat{\Omega}_{\text{EAGL}}$
KLL	45.39 (1.315)	45.18 (1.020)	45.02 (0.835)	154.1 (2.849)	178.4 (2.275)	46.57 (1.179)	46.80 (1.465)
RKLL	61.58 (4.690)	64.58 (2.978)	62.98 (0.962)	132.5 (5.567)	76.36 (1.454)	55.74 (2.360)	46.15 (1.635)
ℓ_2	8.147 (0.310)	8.287 (0.199)	8.269 (0.039)	10.87 (0.145)	9.400 (0.057)	7.946 (0.137)	7.552 (0.159)
ℓ_{sp}	2.474 (0.062)	2.512 (0.039)	2.510 (0.017)	3.028 (0.016)	2.868 (0.009)	2.439 (0.033)	2.381 (0.046)
ℓ_1	4.122 (0.162)	4.197 (0.157)	4.156 (0.155)	4.226 (0.034)	4.074 (0.036)	4.020 (0.158)	3.998 (0.162)
RTE	0.334 (0.034)	0.355 (0.022)	0.352 (0.004)	0.551 (0.016)	0.393 (0.007)	0.298 (0.016)	0.246 (0.020)
uMCC	0.669 (0.006)	0.660 (0.005)	0.664 (0.003)	0.611 (0.004)	0.611 (0.004)	0.680 (0.004)	0.677 (0.004)
BA	0.726 (0.005)	0.727 (0.005)	0.728 (0.005)	0.528 (0.002)	0.528 (0.002)	0.715 (0.006)	0.718 (0.008)

Table 10: Average measures (with standard deviations) over 100 replications for Model 6.

Bold letters indicate the best results.

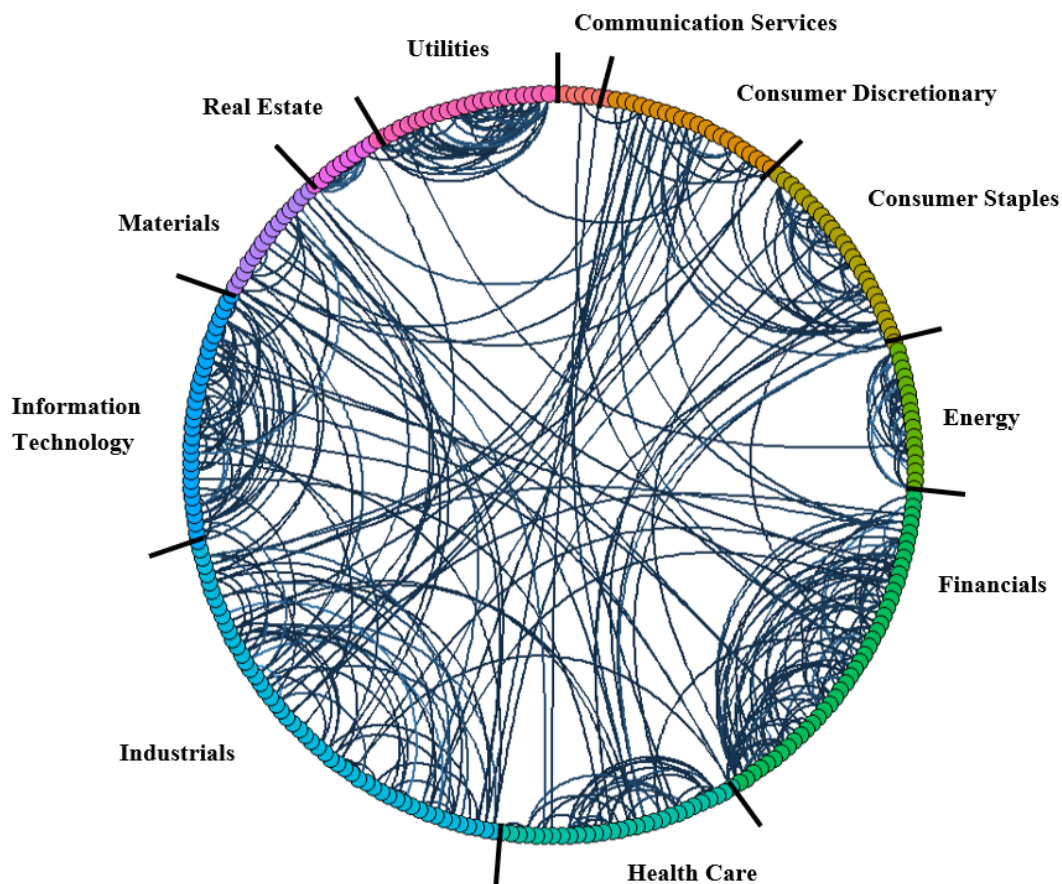
	$\hat{\Omega}_{\text{GLasso}}$	$\hat{\Omega}_{\text{GEN}}$	$\hat{\Omega}_{\text{T-GEN}}$	$\hat{\Omega}_{\text{GRidge}}$	$\hat{\Omega}_{\text{T-GRidge}}$	$\hat{\Omega}_{\text{SCAD}}$	$\hat{\Omega}_{\text{EAGL}}$
KLL	11.43 (0.555)	13.43 (0.532)	7.243 (0.392)	23.27 (1.194)	12.91 (0.391)	9.222 (0.390)	8.613 (0.432)
RKLL	15.25 (0.881)	18.99 (0.827)	8.365 (0.797)	15.27 (2.103)	8.871 (0.849)	10.15 (0.559)	7.977 (0.237)
ℓ_2	4.552 (0.155)	4.817 (0.105)	3.497 (0.148)	4.496 (0.296)	3.616 (0.168)	3.919 (0.085)	3.586 (0.048)
ℓ_{sp}	1.014 (0.047)	1.012 (0.035)	0.771 (0.029)	1.254 (0.031)	1.005 (0.025)	0.976 (0.052)	0.895 (0.041)
ℓ_1	3.436 (0.198)	3.680 (0.203)	3.136 (0.200)	5.768 (0.222)	4.984 (0.156)	3.207 (0.213)	3.135 (0.208)
RTE	0.211 (0.023)	0.238 (0.013)	0.163 (0.016)	0.240 (0.030)	0.164 (0.018)	0.092 (0.021)	0.034 (0.008)
uMCC	0.708 (0.023)	0.639 (0.008)	0.763 (0.017)	0.802 (0.005)	0.782 (0.016)	0.787 (0.015)	0.776 (0.013)
BA	0.831 (0.014)	0.851 (0.010)	0.774 (0.014)	0.686 (0.006)	0.747 (0.005)	0.789 (0.014)	0.796 (0.014)

Table 11: Average measures (with standard deviations) over 100 replications for Model 7.

Bold letters indicate the best results.

	$\hat{\Omega}_{\text{GLasso}}$	$\hat{\Omega}_{\text{GEN}}$	$\hat{\Omega}_{\text{T-GEN}}$	$\hat{\Omega}_{\text{GRidge}}$	$\hat{\Omega}_{\text{T-GRidge}}$	$\hat{\Omega}_{\text{SCAD}}$	$\hat{\Omega}_{\text{EAGL}}$
KLL	13.14 (0.615)	15.57 (0.741)	11.52 (0.598)	25.03 (1.210)	21.08 (0.655)	9.753 (0.817)	9.842 (0.786)
RKLL	16.84 (0.837)	21.10 (1.057)	13.12 (0.747)	20.94 (0.554)	15.15 (0.544)	10.21 (1.045)	8.391 (0.456)
ℓ_2	4.299 (0.140)	4.642 (0.167)	3.952 (0.136)	4.977 (0.053)	4.336 (0.094)	3.198 (0.196)	2.922 (0.084)
ℓ_{sp}	0.974 (0.040)	0.987 (0.032)	0.915 (0.040)	1.135 (0.021)	1.019 (0.016)	0.860 (0.061)	0.846 (0.040)
ℓ_1	3.447 (0.148)	3.729 (0.147)	3.224 (0.165)	3.803 (0.113)	3.600 (0.100)	3.089 (0.189)	3.114 (0.181)
RTE	0.230 (0.018)	0.251 (0.019)	0.223 (0.012)	0.260 (0.001)	0.219 (0.010)	0.085 (0.031)	0.061 (0.007)
uMCC	0.744 (0.019)	0.664 (0.012)	0.798 (0.032)	0.892 (0.011)	0.954 (0.009)	0.804 (0.021)	0.815 (0.007)
BA	0.976 (0.006)	0.945 (0.007)	0.983 (0.005)	0.815 (0.018)	0.969 (0.009)	0.984 (0.003)	0.986 (0.003)

Figure 2: Graphical model representing the interactions between the companies from different sectors. To avoid complexity, the week partial correlations with $|\rho_{ij}| \leq 2sd(NZ)$ are set to zero, where NZ is the vector that contains the non-zero partial correlation entries.



References

- Anderson, T., W. (2003). *An Introduction to Multivariate Statistical Analysis*. Wiley-Interscience.
- Avagyan, V. (2021). D-trace estimation of a precision matrix with eigenvalue control. *Communications in Statistics-Simulation and Computation*, 50(4):1231–1247.
- Avagyan, V., Alonso, A. M., and Nogales, F. J. (2018). D-trace estimation of a precision matrix using adaptive lasso penalties. *Advances in Data Analysis and Classification*, 12(2):425–447.
- Avagyan, V. and Mei, X. (2022). Precision matrix estimation under data contamination with an application to minimum variance portfolio selection. *Communications in Statistics-Simulation and Computation*, 51(4):1381–1400.
- Banerjee, O., El Ghaoui, L., d’Aspremont, A., and Natsoulis, G. (2006). Convex optimization techniques for fitting sparse gaussian graphical models. Proceedings of the 23rd International Conference on Machine Learning.
- Bekker, A., Kheyri, A., and Arashi, M. (2023). A computational note on the graphical ridge in high-dimension. *arXiv preprint arXiv:2312.15781*.
- Bernardini, D., Paterlini, S., and Taufer, E. (2022). New estimation approaches for graphical models with elastic net penalty. *Econometrics and Statistics*.
- Bickel, P., J. and Levina, E. (2008). Regularized estimation of large covariance matrices. *The Annals of Statistics*, 36(1):199–227.
- Bien, J. and Tibshirani, R. J. (2011). Sparse estimation of a covariance matrix. *Biometrika*, 98(4):807–820.

- Bishop, C. M. and Nasrabadi, N. M. (2006). *Pattern recognition and machine learning*. Springer.
- Brodersen, K. H., Ong, C. S., Stephan, K. E., and Buhmann, J. M. (2010). The balanced accuracy and its posterior distribution. In *2010 20th international conference on pattern recognition*.
- Cai, T., Liu, W., and Luo, X. (2011). A constrained ℓ_1 minimization approach to sparse precision matrix estimation. *Journal of the American Statistical Association*, 106(494):594–607.
- Cai, T. T., Li, H., Liu, W., and Xie, J. (2013). Covariate-adjusted precision matrix estimation with an application in genetical genomics. *Biometrika*, 100(1):139–156.
- Chicco, D. and Jurman, G. (2020). The advantages of the matthews correlation coefficient (mcc) over f1 score and accuracy in binary classification evaluation. *BMC Genomics*, 21(1):1–13.
- Choi, Y.-G., Lim, J., and Choi, S. (2019). High-dimensional markowitz portfolio optimization problem: empirical comparison of covariance matrix estimators. *Journal of Statistical Computation and Simulation*, 89(7):1278–1300.
- DeMiguel, V., Garlappi, L., Nogales, F. J., and Uppal, R. (2009a). A generalized approach to portfolio optimization: Improving performance by constraining portfolio norms. *Management Science*, 55(5):798–812.
- DeMiguel, V., Garlappi, L., and Uppal, R. (2009b). Optimal versus naive diversification: How inefficient is the 1/n portfolio strategy? *The Review of Financial Studies*, 22(5):1915–1953.
- Dempster, A. (1972). Covariance selection. *Biometrics*, 28(1):157–175.

- Fan, J., Feng, J., and Wu, Y. (2009). Network exploration via the adaptive lasso and scad penalties. *The Annals of Applied Statistics*, 3(2):521–541.
- Fan, J., Liao, Y., and Liu, H. (2016). An overview of the estimation of large covariance and precision matrices. *The Econometrics Journal*, 19(1):C1–C32.
- Friedman, J., Hastie, T., and Tibshirani, R. (2008). Sparse inverse covariance estimation with the graphical lasso. *Biostatistics*, 9(3):432–441.
- Goto, S. and Xu, Y. (2015). Improving mean variance optimization through sparse hedging restrictions. *Journal of Financial and Quantitative Analysis*, 50(6):1415–1441.
- Haff, L. (1980). Empirical bayes estimation of the multivariate normal covariance matrix. *The Annals of Statistics*, pages 586–597.
- Huang, S., Li, J., Sun, L., Ye, J., Fleisher, A., Wu, T., Chen, K., and Reiman, E. (2010). Learning brain connectivity of alzheimer’s disease by sparse inverse covariance estimation. *NeuroImage*, 50:935–949.
- James, W. and Stein, C. (1992). Estimation with quadratic loss. In *Breakthroughs in statistics: Foundations and basic theory*, pages 443–460. Springer.
- Kovács, S., Ruckstuhl, T., Obrist, H., and Bühlmann, P. (2021). Graphical elastic net and target matrices: Fast algorithms and software for sparse precision matrix estimation. *arXiv preprint arXiv:2101.02148*.
- Kuismin, M., Kemppainen, J., and Sillanpää, M. (2017). Precision matrix estimation with rope. *Journal of Computational and Graphical Statistics*, 26(3):682–694.
- Lauritzen, S. (1996). *Graphical Models*. Clarendon Press. Oxford.
- Ledoit, O. and Wolf, M. (2004). Honey, i shrunk the sample covariance matrix. *The Journal of Portfolio Management*, 30(4):110–119.

- Liu, W. and Luo, X. (2015). Fast and adaptive sparse precision matrix estimation in high dimensions. *Journal of Multivariate Analysis*, 135:153–162.
- Liu, Z., Lin, S., Deng, N., McGovern, D. P., and Piantadosi, S. (2016). Sparse inverse covariance estimation with ℓ_0 penalty for network construction with omics data. *Journal of Computational Biology*, 23(3):192–202.
- Marjanovic, G. and Hero, A. O. (2015). ℓ_0 sparse inverse covariance estimation. *IEEE Transactions on Signal Processing*, 63(12):3218–3231.
- Marjanovic, G. and Solo, V. (2014). On ℓ_q optimization and sparse inverse covariance selection. *IEEE transactions on signal processing*, 62(7):1644–1654.
- Markowitz, H. (1952). Portfolio selection. *Journal of Finance*, 7:77–91.
- Matthews, B. W. (1975). Comparison of the predicted and observed secondary structure of t4 phage lysozyme. *Biochimica et Biophysica Acta*, 405:442–451.
- McLachlan, S. (2004). *Discriminant Analysis and Statistical Pattern Recognition*. Wiley Interscience.
- Meinshausen, N. and Bühlmann, P. (2006). High-dimensional graphs and variable selection with the lasso. *The Annals of Statistics*, 34(2):1436–1462.
- Peeters, C. F., Bilgrau, A. E., and van Wieringen, W. N. (2022). rags2ridges: A one-stop-shop for graphical modeling of high-dimensional precision matrices. *Journal of Statistical Software*, 102(4):1–32.
- Peng, W., Wang, P., Zhou, N., and Zhu, J. (2009). Partial correlation estimation by joint sparse regression models. *Journal of the American Statistical Association*, 104(486):735–746.

- Ravikumar, P., Wainwright, M., Raskutti, G., and Yu, B. (2011). High-dimensional covariance estimation by minimizing ℓ_1 -penalized log-determinant divergence. *Electronic Journal of Statistics*, 5:935–980.
- Rothman, A., Bickel, P., Levina, E., and Zhu, J. (2008). Sparse permutation invariant covariance estimation. *Electronic Journal of Statistics*, 2:494–515.
- Rothman, A. J. (2012). Positive definite estimators of large covariance matrices. *Biometrika*, 99(2):733–740.
- Shannon, C. E. (1948). A mathematical theory of communication. *The Bell System Technical Journal*, 27(3):379–423.
- Singh, D., Febbo, P. G., Ross, K., Jackson, D. G., Manola, J., Ladd, C., Tamayo, P., Renshaw, A. A., D’Amico, A. V., Richie, J. P., et al. (2002). Gene expression correlates of clinical prostate cancer behavior. *Cancer Cell*, 1(2):203–209.
- Stevens, G. V. G. (1998). On the inverse of the covariance matrix in portfolio analysis. *The Journal of Finance*, 53(5):1821–1827.
- Tibshirani, R. (1996). Regression shrinkage and selection via the lasso. *Journal of the Royal Statistical Society Series B: Statistical Methodology*, 58(1):267–288.
- Till, A. C., Florquin, R., Delhaye, M., Kornreich, C., Williams, D. R., and Briganti, G. (2023). A network perspective on abnormal child behavior in primary school students. *Psychological reports*, 126(4):1933–1953.
- van Wieringen, W. N. and Peeters, C. F. (2016). Ridge estimation of inverse covariance matrices from high-dimensional data. *Computational Statistics & Data Analysis*, 103:284–303.
- Wasserman, L. and Roeder, K. (2009). High dimensional variable selection. *The Annals of Statistics*, 37(5A):2178.

- Witten, D. M. and Tibshirani, R. (2009). Covariance-regularized regression and classification for high dimensional problems. *Journal of the Royal Statistical Society Series B: Statistical Methodology*, 71(3):615–636.
- Yin, J. and Li, J. (2013). Adjusting for high-dimensional covariates in sparse precision matrix estimation by ℓ_1 -penalization. *Journal of Multivariate Analysis*, 116:365–381.
- Yuan, M. (2010). High dimensional inverse covariance matrix estimation via linear programming. *Journal of Machine Learning Research*, 11:2261–2286.
- Yuan, M. and Lin, Y. (2007). Model selection and estimation in the gaussian graphical model. *Biometrika*, 94(1):19–35.
- Zhang, T. and Zou, H. (2014). Sparse precision matrix estimation via lasso penalized d-trace loss. *Biometrika*, 88:1–18.
- Zou, H. and Hastie, T. (2005). Regularization and variable selection via the elastic net. *Journal of the Royal Statistical Society Series B: Statistical Methodology*, 67(2):301–320.

Supplementary Materials

A Technical details

Entropy is a crucial scientific concept closely related to uncertainty and randomness. It originates from the field of information theory and is introduced by Shannon (1948). It is borrowed in statistics for understanding the randomness in the data. Suppose \mathbf{X} follows a multivariate Gaussian distribution with mean μ and covariance matrix $\Sigma = \Omega^{-1}$, i.e., $\mathbf{X} \sim N(\mu, \Omega^{-1})$. The entropy of a continuous random variable is defined as:

$$H(\mathbf{X}) = - \int p(\mathbf{X}) \log p(\mathbf{X}) dx, \quad (13)$$

where $p(\mathbf{X})$ probability density function and is defined for the Gaussian distribution as:

$$p(\mathbf{X}) = (2\pi)^{-p/2} \det(\Omega)^{1/2} \exp\left(-\frac{1}{2}(\mathbf{X} - \mu)^T \Omega (\mathbf{X} - \mu)\right) \quad (14)$$

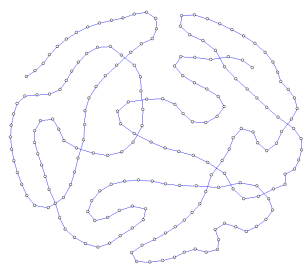
Therefore, we have:

$$\begin{aligned} H(\mathbf{X}) &= -\mathbf{E}[\log(p(\mathbf{X}))] \\ &= -\mathbf{E}\left[\log\left[(2\pi)^{-p/2} \det(\Omega)^{1/2} \exp\left(-\frac{1}{2}(\mathbf{X} - \mu)^T \Omega (\mathbf{X} - \mu)\right)\right]\right] \\ &= \frac{p}{2} \log(2\pi) - \frac{1}{2} \log \det(\Omega) + \frac{1}{2} \mathbf{E}\left[(\mathbf{X} - \mu)^T \Omega (\mathbf{X} - \mu)\right] \\ &= \frac{p}{2} (1 + \log(2\pi)) - \frac{1}{2} \log \det(\Omega) \\ &= \frac{p}{2} (1 + \log(2\pi)) + \frac{1}{2} \log \det(\Omega^{-1}) \\ &= \frac{p}{2} (1 + \log(2\pi)) + \frac{1}{2} H_C(\mathbf{X}) \\ &= C + \frac{1}{2} H_C(\mathbf{X}), \end{aligned}$$

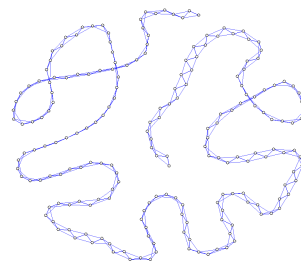
where C is a constant. Here, we used the fact that $\mathbf{E}\left[(\mathbf{X} - \mu)^T \Omega (\mathbf{X} - \mu)\right] = p$.

B Simulation models

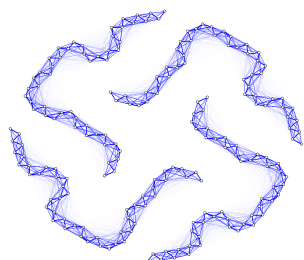
Figure 1: Gaussian Graphical models corresponding to each precision matrix model.



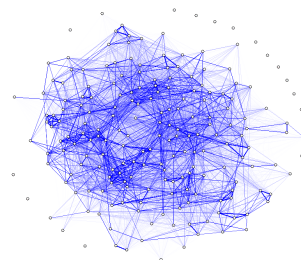
Model 1



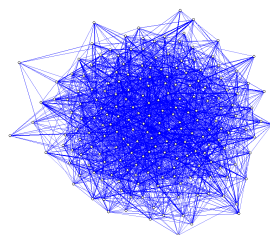
Model 2



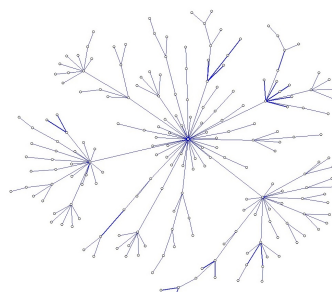
Model 3



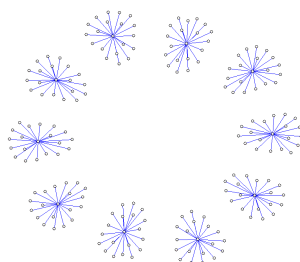
Model 4



Model 5



Model 6



Model 7

C Additional simulation results

In this section, we present additional numerical results based on the same simulation settings described in Section 3, with the penalty parameter γ now selected using the BIC criterion. For a comprehensive comparison, we provide the results for both 5-fold CV and BIC. The results indicate that, in the majority of cases, the precision matrices estimated using CV tend to have lower statistical losses compared to those estimated with BIC. This suggests that CV may offer a more effective approach for obtaining lower statistical losses in these scenarios.

When examining Gaussian Graphical Model (GGM) selection, the results are more mixed. For certain models, such as models 4 and 5, CV leads to higher values for both uMCC and BA, compared to BIC, suggesting better sparsity pattern selection performance. However, in other cases, such as models 2 and 6, CV results in higher BA but lower uMCC than BIC. Therefore, we do not observe a consistent advantage of BIC approach in terms of sparsity prediction measures.

Table 1: Average measures (with standard deviations) over 100 replications for Model 1.

Bold letters indicate the best results.

		$\widehat{\Omega}_{\text{GLasso}}$	$\widehat{\Omega}_{\text{GEN}}$	$\widehat{\Omega}_{\text{T-GEN}}$	$\widehat{\Omega}_{\text{GRidge}}$	$\widehat{\Omega}_{\text{T-GRidge}}$	$\widehat{\Omega}_{\text{SCAD}}$	$\widehat{\Omega}_{\text{EAGL}}$
KLL	BIC	49.11 (4.926)	63.89 (2.843)	53.67 (0.518)	56.65 (1.556)	59.18 (2.177)	36.45 (0.638)	36.71 (2.710)
	CV	27.56 (0.930)	33.08 (0.627)	30.86 (0.541)	58.14 (1.399)	64.03 (2.624)	21.00 (0.591)	23.61 (0.839)
RKLL	BIC	89.66 (12.02)	132.2 (7.750)	94.19 (2.016)	49.01 (0.720)	49.70 (0.799)	58.29 (0.954)	34.87 (2.007)
	CV	38.30 (2.767)	49.72 (1.681)	45.20 (0.918)	75.97 (0.832)	87.32 (5.451)	25.49 (0.745)	22.77 (0.845)
ℓ_2	BIC	10.48 (0.369)	11.54 (0.163)	10.67 (0.060)	8.404 (0.031)	8.427 (0.038)	9.296 (0.042)	7.517 (0.164)
	CV	7.493 (0.401)	8.365 (0.191)	8.193 (0.047)	9.994 (0.019)	10.40 (0.201)	6.318 (0.078)	6.107 (0.153)
ℓ_{sp}	BIC	1.303 (0.034)	1.407 (0.015)	1.333 (0.013)	1.086 (0.018)	1.089 (0.015)	1.190 (0.013)	1.005 (0.018)
	CV	1.041 (0.039)	1.126 (0.019)	1.105 (0.013)	1.253 (0.010)	1.308 (0.025)	0.927 (0.023)	0.891 (0.023)
ℓ_1	BIC	1.472 (0.028)	1.529 (0.021)	1.430 (0.018)	1.223 (0.039)	1.216 (0.032)	1.416 (0.039)	1.219 (0.043)
	CV	1.654 (0.084)	1.775 (0.066)	1.688 (0.053)	1.356 (0.026)	1.395 (0.029)	1.467 (0.068)	1.403 (0.068)
RTE	BIC	0.561 (0.022)	0.624 (0.010)	0.560 (0.006)	0.354 (0.001)	0.346 (0.004)	0.489 (0.003)	0.328 (0.007)
	CV	0.369 (0.030)	0.419 (0.015)	0.410 (0.003)	0.482 (0.001)	0.495 (0.015)	0.297 (0.005)	0.256 (0.010)
uMCC	BIC	0.818 (0.031)	0.835 (0.017)	0.894 (0.008)	0.983 (0.005)	0.976 (0.009)	0.787 (0.006)	0.842 (0.019)
	CV	0.653 (0.011)	0.634 (0.002)	0.648 (0.002)	0.979 (0.007)	0.955 (0.018)	0.681 (0.003)	0.704 (0.004)
BA	BIC	0.988 (0.003)	0.990 (0.002)	0.994 (0.001)	0.989 (0.005)	0.991 (0.006)	0.985 (0.001)	0.991 (0.002)
	CV	0.936 (0.009)	0.919 (0.002)	0.933 (0.002)	0.990 (0.006)	0.990 (0.008)	0.955 (0.002)	0.965 (0.001)

Table 2: Average measures (with standard deviations) over 100 replications for Model 2.

Bold letters indicate the best results.

		$\hat{\Omega}_{\text{GLasso}}$	$\hat{\Omega}_{\text{GEN}}$	$\hat{\Omega}_{\text{T-GEN}}$	$\hat{\Omega}_{\text{GRidge}}$	$\hat{\Omega}_{\text{T-GRidge}}$	$\hat{\Omega}_{\text{SCAD}}$	$\hat{\Omega}_{\text{EAGL}}$
KLL	BIC	75.61 (4.260)	84.73 (2.809)	70.54 (1.776)	69.66 (1.576)	71.54 (1.886)	68.91 (1.495)	66.71 (1.902)
	CV	45.05 (1.137)	47.27 (0.629)	46.80 (0.706)	69.07 (1.931)	77.36 (0.849)	42.08 (1.267)	46.07 (1.135)
RKLL	BIC	203.5 (17.52)	250.6 (13.05)	159.0 (3.829)	135.5 (2.541)	96.57 (1.708)	170.8 (5.746)	90.29 (0.762)
	CV	77.94 (6.640)	84.77 (0.981)	85.06 (3.230)	106.7 (3.601)	162.0 (2.687)	63.59 (5.960)	58.75 (1.691)
ℓ_2	BIC	14.79 (0.185)	15.24 (0.113)	14.25 (0.056)	13.83 (0.043)	12.85 (0.048)	14.41 (0.069)	12.68 (0.021)
	CV	11.92 (0.393)	12.17 (0.029)	12.29 (0.180)	13.15 (0.085)	14.31 (0.040)	11.27 (0.374)	11.21 (0.147)
ℓ_{sp}	BIC	2.313 (0.021)	2.361 (0.013)	2.253 (0.009)	2.181 (0.010)	2.059 (0.012)	2.271 (0.009)	2.059 (0.009)
	CV	1.954 (0.054)	1.984 (0.010)	2.002 (0.025)	2.096 (0.014)	2.247 (0.006)	1.875 (0.054)	1.867 (0.023)
ℓ_1	BIC	2.452 (0.020)	2.462 (0.015)	2.382 (0.021)	2.310 (0.022)	2.212 (0.027)	2.443 (0.024)	2.307 (0.036)
	CV	2.683 (0.067)	2.773 (0.043)	2.695 (0.050)	2.250 (0.027)	2.325 (0.014)	2.602 (0.058)	2.547 (0.060)
RTE	BIC	0.646 (0.011)	0.682 (0.007)	0.585 (0.006)	0.560 (0.001)	0.448 (0.004)	0.616 (0.005)	0.419 (0.004)
	CV	0.467 (0.028)	0.484 (0.002)	0.489 (0.013)	0.493 (0.007)	0.573 (0.005)	0.412 (0.026)	0.366 (0.010)
uMCC	BIC	0.822 (0.008)	0.827 (0.007)	0.829 (0.006)	0.871 (0.009)	0.866 (0.008)	0.817 (0.005)	0.817 (0.005)
	CV	0.671 (0.011)	0.651 (0.002)	0.668 (0.006)	0.873 (0.008)	0.827 (0.007)	0.689 (0.009)	0.703 (0.007)
BA	BIC	0.892 (0.025)	0.873 (0.018)	0.861 (0.018)	0.830 (0.017)	0.830 (0.015)	0.913 (0.011)	0.914 (0.008)
	CV	0.919 (0.010)	0.900 (0.002)	0.917 (0.005)	0.829 (0.016)	0.795 (0.014)	0.933 (0.005)	0.940 (0.004)

Table 3: Average measures (with standard deviations) over 100 replications for Model 3.

Bold letters indicate the best results.

		$\widehat{\Omega}_{\text{GLasso}}$	$\widehat{\Omega}_{\text{GEN}}$	$\widehat{\Omega}_{\text{T-GEN}}$	$\widehat{\Omega}_{\text{GRidge}}$	$\widehat{\Omega}_{\text{T-GRidge}}$	$\widehat{\Omega}_{\text{SCAD}}$	$\widehat{\Omega}_{\text{EAGL}}$
KLL	BIC	52.57 (0.767)	58.64 (0.327)	43.46 (0.432)	41.85 (0.878)	45.48 (0.942)	44.87 (3.644)	46.53 (2.486)
	CV	37.53 (0.736)	40.05 (0.420)	37.814 (0.401)	51.628 (0.608)	56.159 (0.231)	34.445 (0.673)	37.047 (0.778)
RKLL	BIC	158.2 (3.365)	189.0 (1.541)	111.0 (1.337)	86.20 (1.480)	80.51 (1.174)	122.1 (15.86)	77.41 (3.666)
	CV	86.52 (5.332)	95.22 (1.214)	92.807 (1.594)	155.85 (2.930)	144.915 (2.111)	72.145 (3.845)	61.52 (0.917)
ℓ_2	BIC	16.48 (0.050)	16.85 (0.016)	15.68 (0.029)	15.01 (0.039)	14.76 (0.038)	15.87 (0.300)	14.61 (0.138)
	CV	14.87 (0.214)	15.10 (0.028)	15.218 (0.044)	16.479 (0.043)	16.312 (0.033)	14.396 (0.166)	13.93 (0.047)
ℓ_{sp}	BIC	3.480 (0.008)	3.529 (0.004)	3.368 (0.008)	3.262 (0.008)	3.216 (0.008)	3.395 (0.043)	3.192 (0.019)
	CV	3.249 (0.033)	3.280 (0.008)	3.299 (0.008)	3.477 (0.007)	3.448 (0.005)	3.180 (0.026)	3.096 (0.011)
ℓ_1	BIC	3.630 (0.019)	3.658 (0.016)	3.526 (0.015)	3.441 (0.022)	3.389 (0.021)	3.608 (0.029)	3.417 (0.032)
	CV	3.849 (0.078)	3.942 (0.051)	3.673 (0.043)	3.602 (0.014)	3.525 (0.008)	3.758 (0.064)	3.601 (0.057)
RTE	BIC	0.607 (0.004)	0.641 (0.002)	0.523 (0.006)	0.441 (0.001)	0.391 (0.004)	0.557 (0.021)	0.371 (0.005)
	CV	0.495 (0.018)	0.514 (0.003)	0.515 (0.005)	0.603 (0.005)	0.523 (0.006)	0.447 (0.015)	0.359 (0.005)
uMCC	BIC	0.590 (0.003)	0.590 (0.002)	0.590 (0.002)	0.599 (0.001)	0.598 (0.001)	0.579 (0.009)	0.587 (0.007)
	CV	0.538 (0.005)	0.532 (0.004)	0.550 (0.004)	0.599 (0.001)	0.594 (0.001)	0.543 (0.004)	0.550 (0.004)
BA	BIC	0.527 (0.001)	0.528 (0.001)	0.528 (0.001)	0.526 (0.001)	0.526 (0.001)	0.528 (0.001)	0.528 (0.001)
	CV	0.527 (0.003)	0.527 (0.003)	0.528 (0.002)	0.526 (0.001)	0.524 (0.001)	0.528 (0.002)	0.528 (0.002)

Table 4: Average measures (with standard deviations) over 100 replications for Model 4.

Bold letters indicate the best results.

		$\widehat{\Omega}_{\text{GLasso}}$	$\widehat{\Omega}_{\text{GEN}}$	$\widehat{\Omega}_{\text{T-GEN}}$	$\widehat{\Omega}_{\text{GRidge}}$	$\widehat{\Omega}_{\text{T-GRidge}}$	$\widehat{\Omega}_{\text{SCAD}}$	$\widehat{\Omega}_{\text{EAGL}}$
KLL	BIC	132.9 (5.040)	141.4 (4.639)	145.6 (3.649)	137.1 (2.930)	138.6 (2.934)	133.1 (4.732)	132.8 (3.981)
	CV	92.70 (1.535)	95.88 (0.995)	95.19 (1.002)	135.1 (2.476)	135.4 (1.873)	91.84 (1.019)	107.9 (1.891)
RKLL	BIC	716.2 (57.46)	783.4 (55.54)	791.5 (35.23)	257.8 (2.257)	248.1 (2.498)	718.6 (53.93)	202.0 (3.505)
	CV	259.6 (22.24)	267.8 (1.860)	261.9 (1.884)	289.5 (8.626)	357.9 (2.342)	264.4 (10.01)	155.8 (4.080)
ℓ_2	BIC	19.10 (0.107)	19.27 (0.088)	19.31 (0.059)	17.51 (0.012)	17.41 (0.013)	19.10 (0.101)	16.62 (0.038)
	CV	17.26 (0.205)	17.41 (0.013)	17.36 (0.014)	17.78 (0.054)	18.23 (0.011)	17.28 (0.107)	15.94 (0.077)
ℓ_{sp}	BIC	5.478 (0.010)	5.484 (0.009)	5.473 (0.005)	5.202 (0.007)	5.190 (0.007)	5.478 (0.009)	5.248 (0.010)
	CV	5.291 (0.024)	5.291 (0.008)	5.287 (0.008)	5.236 (0.008)	5.292 (0.005)	5.303 (0.014)	5.150 (0.017)
ℓ_1	BIC	10.35 (0.028)	10.37 (0.026)	10.37 (0.024)	9.961 (0.049)	9.944 (0.049)	10.36 (0.028)	9.994 (0.058)
	CV	10.11 (0.061)	10.11 (0.056)	10.10 (0.057)	10.01 (0.045)	10.10 (0.039)	10.11 (0.056)	9.913 (0.080)
RTE	BIC	0.811 (0.010)	0.831 (0.008)	0.836 (0.005)	0.688 (0.001)	0.678 (0.001)	0.812 (0.009)	0.508 (0.003)
	CV	0.654 (0.017)	0.678 (0.002)	0.672 (0.002)	0.713 (0.005)	0.752 (0.001)	0.649 (0.010)	0.481 (0.006)
uMCC	BIC	0.586 (0.003)	0.586 (0.003)	0.581 (0.003)	0.590 (0.002)	0.591 (0.002)	0.586 (0.003)	0.592 (0.003)
	CV	0.597 (0.003)	0.597 (0.003)	0.598 (0.003)	0.591 (0.002)	0.594 (0.002)	0.598 (0.003)	0.598 (0.003)
BA	BIC	0.545 (0.004)	0.544 (0.003)	0.537 (0.003)	0.532 (0.001)	0.532 (0.001)	0.544 (0.003)	0.555 (0.003)
	CV	0.580 (0.003)	0.583 (0.003)	0.583 (0.003)	0.532 (0.001)	0.536 (0.002)	0.578 (0.002)	0.578 (0.003)

Table 5: Average measures (with standard deviations) over 100 replications for Model 5.

Bold letters indicate the best results.

		$\hat{\Omega}_{\text{GLasso}}$	$\hat{\Omega}_{\text{GEN}}$	$\hat{\Omega}_{\text{T-GEN}}$	$\hat{\Omega}_{\text{GRidge}}$	$\hat{\Omega}_{\text{T-GRidge}}$	$\hat{\Omega}_{\text{SCAD}}$	$\hat{\Omega}_{\text{EAGL}}$
KLL	BIC	76.20 (5.512)	87.71 (6.936)	106.05 (3.101)	149.8 (1.073)	139.7 (1.820)	57.99 (3.468)	71.23 (4.913)
	CV	45.39 (1.315)	45.18 (1.020)	45.02 (0.835)	154.1 (2.849)	178.4 (2.275)	46.57 (1.179)	46.80 (1.465)
RKLL	BIC	152.5 (16.89)	195.3 (21.95)	195.4 (12.77)	199.5 (0.672)	173.1 (9.354)	93.04 (9.484)	65.86 (1.833)
	CV	61.58 (4.690)	64.58 (2.978)	62.98 (0.962)	132.5 (5.567)	76.36 (1.454)	55.74 (2.360)	46.15 (1.635)
ℓ_2	BIC	10.95 (0.273)	11.58 (0.256)	11.61 (0.140)	11.82 (0.009)	11.50 (0.121)	9.610 (0.298)	8.766 (0.078)
	CV	8.147 (0.310)	8.287 (0.199)	8.269 (0.039)	10.87 (0.145)	9.400 (0.057)	7.946 (0.137)	7.552 (0.159)
ℓ_{sp}	BIC	2.956 (0.041)	3.038 (0.036)	3.065 (0.016)	3.117 (0.004)	3.077 (0.011)	2.754 (0.051)	2.704 (0.024)
	CV	2.474 (0.062)	2.512 (0.039)	2.510 (0.017)	3.028 (0.016)	2.868 (0.009)	2.439 (0.033)	2.381 (0.046)
ℓ_1	BIC	4.305 (0.091)	4.372 (0.083)	4.407 (0.110)	4.307 (0.031)	4.246 (0.027)	4.155 (0.106)	4.214 (0.160)
	CV	4.122 (0.162)	4.197 (0.157)	4.156 (0.155)	4.226 (0.034)	4.074 (0.036)	4.020 (0.158)	3.998 (0.162)
RTE	BIC	0.583 (0.022)	0.637 (0.020)	0.630 (0.013)	0.642 (0.001)	0.615 (0.011)	0.465 (0.027)	0.348 (0.006)
	CV	0.334 (0.034)	0.355 (0.022)	0.352 (0.004)	0.551 (0.016)	0.393 (0.007)	0.298 (0.016)	0.246 (0.020)
uMCC	BIC	0.659 (0.007)	0.651 (0.008)	0.615 (0.005)	0.615 (0.005)	0.639 (0.004)	0.674 (0.005)	0.647 (0.007)
	CV	0.669 (0.006)	0.660 (0.005)	0.664 (0.003)	0.611 (0.004)	0.611 (0.004)	0.680 (0.004)	0.677 (0.004)
BA	BIC	0.648 (0.012)	0.641 (0.014)	0.566 (0.006)	0.530 (0.002)	0.554 (0.005)	0.678 (0.010)	0.626 (0.011)
	CV	0.726 (0.005)	0.727 (0.005)	0.728 (0.005)	0.528 (0.002)	0.528 (0.002)	0.715 (0.006)	0.718 (0.008)

Table 6: Average measures (with standard deviations) over 100 replications for Model 6.

Bold letters indicate the best results.

		$\hat{\Omega}_{\text{GLasso}}$	$\hat{\Omega}_{\text{GEN}}$	$\hat{\Omega}_{\text{T-GEN}}$	$\hat{\Omega}_{\text{GRidge}}$	$\hat{\Omega}_{\text{T-GRidge}}$	$\hat{\Omega}_{\text{SCAD}}$	$\hat{\Omega}_{\text{EAGL}}$
KLL	BIC	13.68 (0.505)	21.59 (1.415)	8.404 (0.553)	22.68 (1.165)	13.15 (0.609)	7.783 (0.366)	7.279 (0.493)
	CV	11.43 (0.555)	13.43 (0.532)	7.243 (0.392)	23.27 (1.194)	12.91 (0.391)	9.222 (0.390)	8.613 (0.432)
RKLL	BIC	19.04 (0.737)	32.27 (2.449)	9.360 (1.114)	13.50 (0.141)	7.694 (0.524)	9.186 (0.433)	6.353 (0.184)
	CV	15.25 (0.881)	18.99 (0.827)	8.365 (0.797)	15.27 (2.103)	8.871 (0.849)	10.15 (0.559)	7.977 (0.237)
ℓ_2	BIC	4.880 (0.075)	5.971 (0.170)	3.613 (0.175)	4.281 (0.020)	3.351 (0.120)	3.576 (0.072)	3.070 (0.031)
	CV	4.552 (0.155)	4.817 (0.105)	3.497 (0.148)	4.496 (0.296)	3.616 (0.168)	3.919 (0.085)	3.586 (0.048)
ℓ_{sp}	BIC	1.005 (0.020)	1.087 (0.024)	0.806 (0.023)	1.240 (0.030)	0.918 (0.020)	0.884 (0.027)	0.818 (0.028)
	CV	1.014 (0.047)	1.012 (0.035)	0.771 (0.029)	1.254 (0.031)	1.005 (0.025)	0.976 (0.052)	0.895 (0.041)
ℓ_1	BIC	3.932 (0.170)	4.387 (0.151)	3.065 (0.162)	5.764 (0.227)	4.024 (0.111)	3.286 (0.206)	2.931 (0.179)
	CV	3.436 (0.198)	3.680 (0.203)	3.136 (0.200)	5.768 (0.222)	4.984 (0.156)	3.207 (0.213)	3.135 (0.208)
RTE	BIC	0.278 (0.007)	0.373 (0.014)	0.169 (0.018)	0.221 (0.001)	0.133 (0.015)	0.122 (0.011)	0.031 (0.007)
	CV	0.211 (0.023)	0.238 (0.013)	0.163 (0.016)	0.240 (0.030)	0.164 (0.018)	0.092 (0.021)	0.034 (0.008)
uMCC	BIC	0.777 (0.007)	0.771 (0.010)	0.812 (0.008)	0.801 (0.005)	0.840 (0.004)	0.777 (0.007)	0.800 (0.009)
	CV	0.708 (0.023)	0.639 (0.008)	0.763 (0.017)	0.802 (0.005)	0.782 (0.016)	0.787 (0.015)	0.776 (0.013)
BA	BIC	0.765 (0.006)	0.768 (0.009)	0.736 (0.002)	0.685 (0.006)	0.735 (0.005)	0.765 (0.006)	0.739 (0.005)
	CV	0.831 (0.014)	0.851 (0.010)	0.774 (0.014)	0.686 (0.006)	0.747 (0.005)	0.789 (0.014)	0.796 (0.014)

Table 7: Average measures (with standard deviations) over 100 replications for Model 7.

Bold letters indicate the best results.

		$\hat{\Omega}_{\text{GLasso}}$	$\hat{\Omega}_{\text{GEN}}$	$\hat{\Omega}_{\text{T-GEN}}$	$\hat{\Omega}_{\text{GRidge}}$	$\hat{\Omega}_{\text{T-GRidge}}$	$\hat{\Omega}_{\text{SCAD}}$	$\hat{\Omega}_{\text{EAGL}}$
KLL	BIC	19.27 (1.496)	27.51 (0.994)	15.07 (0.910)	24.848 (1.504)	19.50 (1.157)	11.89 (0.898)	13.058 (1.210)
	CV	13.14 (0.615)	15.57 (0.741)	11.52 (0.598)	25.03 (1.210)	21.08 (0.655)	9.753 (0.817)	9.842 (0.786)
RKLL	BIC	26.58 (2.464)	41.24 (1.744)	16.66 (1.040)	14.01 (0.496)	11.19 (0.395)	13.78 (1.054)	10.63 (0.740)
	CV	16.84 (0.837)	21.10 (1.057)	13.12 (0.747)	20.94 (0.554)	15.15 (0.544)	10.21 (1.045)	8.391 (0.456)
ℓ_2	BIC	5.406 (0.195)	6.499 (0.094)	4.470 (0.120)	3.933 (0.074)	3.519 (0.071)	3.837 (0.147)	3.317 (0.112)
	CV	4.299 (0.140)	4.642 (0.167)	3.952 (0.136)	4.977 (0.053)	4.336 (0.094)	3.198 (0.196)	2.922 (0.084)
ℓ_{sp}	BIC	1.154 (0.043)	1.239 (0.027)	1.087 (0.041)	1.039 (0.023)	0.952 (0.027)	1.006 (0.043)	0.987 (0.046)
	CV	0.974 (0.040)	0.987 (0.032)	0.915 (0.040)	1.135 (0.021)	1.019 (0.016)	0.860 (0.061)	0.846 (0.040)
ℓ_1	BIC	3.648 (0.149)	3.827 (0.111)	3.517 (0.184)	3.715 (0.124)	3.383 (0.141)	3.330 (0.177)	3.407 (0.204)
	CV	3.447 (0.148)	3.729 (0.147)	3.224 (0.165)	3.803 (0.113)	3.600 (0.100)	3.089 (0.189)	3.114 (0.181)
RTE	BIC	0.319 (0.014)	0.406 (0.007)	0.246 (0.011)	0.140 (0.002)	0.130 (0.008)	0.171 (0.013)	0.081 (0.007)
	CV	0.230 (0.018)	0.251 (0.019)	0.223 (0.012)	0.260 (0.001)	0.219 (0.010)	0.085 (0.031)	0.061 (0.007)
uMCC	BIC	0.879 (0.017)	0.869 (0.011)	0.933 (0.010)	0.878 (0.011)	0.936 (0.008)	0.874 (0.011)	0.917 (0.013)
	CV	0.744 (0.019)	0.664 (0.012)	0.798 (0.032)	0.892 (0.011)	0.954 (0.009)	0.804 (0.021)	0.815 (0.007)
BA	BIC	0.987 (0.004)	0.987 (0.004)	0.979 (0.007)	0.792 (0.018)	0.891 (0.015)	0.988 (0.004)	0.983 (0.006)
	CV	0.976 (0.006)	0.945 (0.007)	0.983 (0.005)	0.815 (0.018)	0.969 (0.009)	0.984 (0.003)	0.986 (0.003)

D Asymptotic analysis

In this section, we analyze the convergence rate of the proposed estimator $\widehat{\Omega}_{\text{EAGL}}$. We make the following assumptions to guarantee the existence of the true precision matrix Ω :

$$A1 : \lambda_{\min}(\Omega) \geq \underline{\lambda} > 0,$$

$$A2 : \lambda_{\max}(\Omega) \leq \bar{\lambda},$$

where $\lambda_{\min}(\Omega)$ and $\lambda_{\max}(\Omega)$ are the smallest and largest eigenvalues of Ω , respectively, and $\bar{\lambda}$ and $\underline{\lambda}$ are some positive values. We define the support set $S = \{(i, j) : \Omega_{ij} \neq 0\}$ and assume that $\text{card}(S) \leq s$.

Under the assumptions A1 and A2, if $\gamma \asymp \sqrt{\frac{\log p}{n}}$, then

$$\|\widehat{\Omega}_{\text{EAGL}} - \Omega\|_2 = O_P \left(\sqrt{\frac{(p+s) \log p}{n}} \right), \quad (15)$$

under the standard asymptotics (i.e., assuming that p remains fixed, while n converges to infinity).

The proof of (15) is motivated by Rothman et al. (2008). First, we rewrite the optimization problem of our proposed methodology as:

$$\widehat{\Omega}_{\text{EAGL}} = \arg \min_{\Omega} - (1 + (1 - \alpha)\gamma) \log \det(\Omega) + \text{trace}(\Omega S) + \gamma \alpha \|\Omega\|_1. \quad (16)$$

Consider the following function:

$$\begin{aligned} Q(\Theta) &= - (1 + (1 - \alpha)\gamma) \log \det(\Theta) + \text{trace}(\Theta S) + \gamma \alpha \|\Theta\|_1 - \\ &\quad - (- (1 + (1 - \alpha)\gamma) \log \det(\Omega) + \text{trace}(\Omega S) + \gamma \alpha \|\Omega\|_1) \\ &= - (1 + (1 - \alpha)\gamma) (\log \det(\Theta) - \log \det(\Omega)) + \text{trace}(\Theta - \Omega) S + \gamma \alpha (\|\Theta\|_1 - \|\Omega\|_1), \end{aligned}$$

where Ω is the true precision matrix. Note that the estimator $\widehat{\Omega}_{\text{EAGL}}$ minimizes the function $Q(\Theta)$. This means that the difference matrix $\widehat{\Delta} = \widehat{\Omega}_{\text{EAGL}} - \Omega$ minimizes the function $G(\Delta) = Q(\Omega + \Delta)$. Moreover, $G(\widehat{\Delta}) \leq G(0) = Q(\Omega) = 0$ and $G(\Delta)$ is a convex function.

Define the following set:

$$\Phi_n(M) = \{\Delta : \Delta = \Delta^T, \|\Delta\|_2 = Mr_n\},$$

where $r_n = \sqrt{\frac{(p+s)\log p}{n}} \rightarrow 0$. If we show that $\inf\{G(\Delta) : \Delta \in \Phi_n(M)\} > 0$, then the minimizer $\hat{\Delta}$ must be inside the sphere defined by $\Phi_n(M)$, i.e., $\|\hat{\Delta}\|_2 \leq Mr_n$.

$$\begin{aligned} G(\Delta) &= Q(\Omega + \Delta) = -(1 + (1 - \alpha)\gamma) (\log \det(\Omega + \Delta) - \log \det(\Omega)) \\ &+ \text{trace}(\Omega + \Delta - \Omega)S + \gamma\alpha (\|\Omega + \Delta\|_1 - \|\Omega\|_1) \\ &= -(1 + (1 - \alpha)\gamma) (\log \det(\Omega + \Delta) - \log \det(\Omega)) + \text{trace}(S - \Sigma)\Delta \\ &+ \text{trace}\Sigma\Delta + \gamma\alpha (\|\Omega + \Delta\|_1 - \|\Omega\|_1) \end{aligned} \quad (17)$$

From the Taylor expansion of the function $g(t) = \log \det(\Omega + t\Delta)$, we get that:

$$\begin{aligned} \log \det(\Omega + \Delta) - \log \det(\Omega) &= \text{trace}(\Omega^{-1}\Delta) - \\ &\text{vec}(\Delta)^T \left[\int_0^1 (1 - \tau)(\Omega + \tau\Delta)^{-1} \otimes (\Omega + \tau\Delta)^{-1} d\tau \right] \text{vec}(\Delta), \end{aligned}$$

where \otimes is the Kronecker product, and $\text{vec}(\Delta)$ is a vectorization of matrix Δ . For $\Delta \in \Phi_n(M)$, we have:

$$\begin{aligned} \text{vec}(\Delta)^T \left[\int_0^1 (1 - \tau)(\Omega + \tau\Delta)^{-1} \otimes (\Omega + \tau\Delta)^{-1} d\tau \right] \text{vec}(\Delta) &\geq \\ \lambda_{\min} \left(\int_0^1 (1 - \tau)(\Omega + \tau\Delta)^{-1} \otimes (\Omega + \tau\Delta)^{-1} d\tau \right) \|\Delta\|_2^2 &\geq \\ \int_0^1 (1 - \tau)\lambda_{\min}^2(\Omega + \tau\Delta)^{-1} d\tau \|\Delta\|_2^2 &\geq \frac{1}{2} \min_{0 \leq \tau \leq 1} \lambda_{\min}^2(\Omega + \tau\Delta)^{-1} \|\Delta\|_2^2. \end{aligned} \quad (18)$$

Furthermore:

$$\min_{0 \leq \tau \leq 1} \lambda_{\min}^2(\Omega + \tau\Delta)^{-1} \geq \lambda_{\max}^{-2}(\Omega + \Delta) \geq (\|\Omega\|_{\text{sp}} + \|\Delta\|_{\text{sp}})^{-2} \geq \frac{1}{\bar{\lambda} + \|\Delta\|_{\text{sp}}^2} \geq \frac{1}{2}\bar{\lambda}^{-2}, \quad (19)$$

since $\|\Delta\|_{\text{sp}} \leq \|\Delta\|_2 = o(1)$, with probability tending to 1.

The equation (17) can be rewritten in the following form:

$$\begin{aligned}
G(\Delta) = & -(1 + (1 - \alpha)\gamma) \left(\text{trace}\Sigma\Delta - \frac{1}{4}\bar{\lambda}^{-2}\|\Delta\|_2^2 \right) + \\
& \text{trace}(\Delta(S - \Sigma)) + \text{trace}(\Sigma\Delta) + \gamma\alpha(\|\Omega + \Delta\|_1 - \|\Omega\|_1) = \\
& (1 + (1 - \alpha)\gamma) \frac{1}{4}\bar{\lambda}^{-2}\|\Delta\|_2^2 - (1 - \alpha)\gamma\text{trace}\Sigma\Delta + \\
& \text{trace}(\Delta(S - \Sigma)) + \gamma\alpha(\|\Omega + \Delta\|_1 - \|\Omega\|_1). \quad (20)
\end{aligned}$$

For an index set S and a matrix $A = [a_{ij}]$, we denote $A_S = [a_{ij}I((i, j) \in S)]$, where $I(\cdot)$ is an indicator function. Recall $S = \{(i, j) : \Omega_{ij} \neq 0\}$, and \bar{S} is its complement. It is straightforward that $\|\Omega_{\bar{S}}\|_1 = 0$. From the triangular inequality, we have

$$\begin{aligned}
\|\Omega + \Delta\|_1 - \|\Omega\|_1 &= \|\Omega_S + \Delta_S\|_1 + \|\Delta_{\bar{S}}\|_1 - \|\Omega_S\|_1 \geq \\
& \|\Omega_S\|_1 - \|\Delta_S\|_1 + \|\Delta_{\bar{S}}\|_1 - \|\Omega_S\|_1 = \|\Delta_{\bar{S}}\|_1 - \|\Delta_S\|_1
\end{aligned}$$

Next, we consider the term $\text{trace}(\Delta(S - \Sigma))$. Following the results of Bickel and Levina (2008), we obtain:

$$\text{trace}(\Delta(S - \Sigma)) \leq \|S - \Sigma\|_\infty \|\Delta\|_1 = O_P\left(\sqrt{\frac{\log p}{n}}\right) \|\Delta\|_1 \leq C_1 \sqrt{\frac{\log p}{n}} \|\Delta\|_1,$$

with probability tending to 1, where C_1 is some positive value. Note that $\|\Delta\|_1 = \|\Delta_{\bar{S}}\|_1 + \|\Delta_S\|_1$.

The lower bound of the term $\text{trace}\Sigma\Delta$ is obtained using Cauchy-Schwartz inequality:

$$\text{trace}\Sigma\Delta \leq \|\Sigma\|_2 \|\Delta\|_2, \quad (21)$$

also with probability tending to 1. Now, take $\gamma = \frac{C_1}{\epsilon} \sqrt{\frac{\log p}{n}}$, where ϵ is a small positive

value. Combining the obtained lower bounds, we get from (20):

$$\begin{aligned}
G(\Delta) &\geq \left(1 + (1 - \alpha) \frac{C_1}{\epsilon} \sqrt{\frac{\log p}{n}}\right) \frac{1}{4} \bar{\lambda}^{-2} \|\Delta\|_2^2 - (1 - \alpha) \frac{C_1}{\epsilon} \sqrt{\frac{\log p}{n}} \|\Sigma\|_2 \|\Delta\|_2 - \\
&\quad C_1 \sqrt{\frac{\log p}{n}} (\|\Delta_{\bar{S}}\|_1 + \|\Delta_S\|_1) + \frac{C_1}{\epsilon} \sqrt{\frac{\log p}{n}} \alpha (\|\Delta_{\bar{S}}\|_1 - \|\Delta_S\|_1) = \\
&\quad \left(1 + (1 - \alpha) \frac{C_1}{\epsilon} \sqrt{\frac{\log p}{n}}\right) \frac{1}{4} \bar{\lambda}^{-2} \|\Delta\|_2^2 - (1 - \alpha) \frac{C_1}{\epsilon} \sqrt{\frac{\log p}{n}} \|\Sigma\|_2 \|\Delta\|_2 - \\
&\quad \|\Delta_{\bar{S}}\|_1 C_1 \sqrt{\frac{\log p}{n}} \left(1 - \frac{\alpha}{\epsilon}\right) - \|\Delta_S\|_1 C_1 \sqrt{\frac{\log p}{n}} \left(1 + \frac{\alpha}{\epsilon}\right) \geq \\
&\quad \left(1 + (1 - \alpha) C_1 \sqrt{\frac{\log p}{n}}\right) \frac{1}{4} \bar{\lambda}^{-2} \|\Delta\|_2^2 - (1 - \alpha) C_1 \sqrt{\frac{\log p}{n}} \|\Sigma\|_2 \|\Delta\|_2 - \|\Delta_S\|_1 C_1 \sqrt{\frac{\log p}{n}} \left(1 + \frac{\alpha}{\epsilon}\right).
\end{aligned}$$

Note that $\|\Delta_S\|_1 \leq \sqrt{s} \|\Delta_S\|_2 \leq \sqrt{s} \|\Delta\|_2$, which gives us

$$\begin{aligned}
G(\Delta) &\geq \left(1 + (1 - \alpha) \frac{C_1}{\epsilon} \sqrt{\frac{\log p}{n}}\right) \frac{1}{4} \bar{\lambda}^{-2} \|\Delta\|_2^2 - (1 - \alpha) \frac{C_1}{\epsilon} \sqrt{\frac{\log p}{n}} \|\Sigma\|_2 \|\Delta\|_2 - \\
&\quad C_1 \sqrt{\frac{s \log p}{n}} \left(1 + \frac{\alpha}{\epsilon}\right) \|\Delta\|_2 \geq \\
&\quad \|\Delta\|_2^2 \left(\left(1 + (1 - \alpha) \frac{C_1}{\epsilon} \sqrt{\frac{\log p}{n}}\right) \frac{1}{4} \bar{\lambda}^{-2} - (1 - \alpha) \frac{C_1}{\epsilon} \sqrt{\frac{(s+p) \log p}{n}} \|\Sigma\|_2 \|\Delta\|_2^{-1} - \right. \\
&\quad \left. C_1 \sqrt{\frac{(s+p) \log p}{n}} \left(1 + \frac{\alpha}{\epsilon}\right) \|\Delta\|_2^{-1} \right) = \|\Delta\|_2^2 \left(\left(1 + (1 - \alpha) \frac{C_1}{\epsilon} \sqrt{\frac{\log p}{n}}\right) \frac{1}{4} \bar{\lambda}^{-2} - \right. \\
&\quad \left. (1 - \alpha) \frac{C_1}{M \epsilon} \|\Sigma\|_2 - \frac{C_1}{M} \left(1 + \frac{\alpha}{\epsilon}\right) \right),
\end{aligned}$$

which is positive for a sufficiently large M . This establishes the convergence rate (15).

An open question remains regarding the degree of stringency of the positivity of $G(\Delta)$ depending on α and the limitations on $\|\Sigma\|_2$. We leave this problem to be studied in the future.